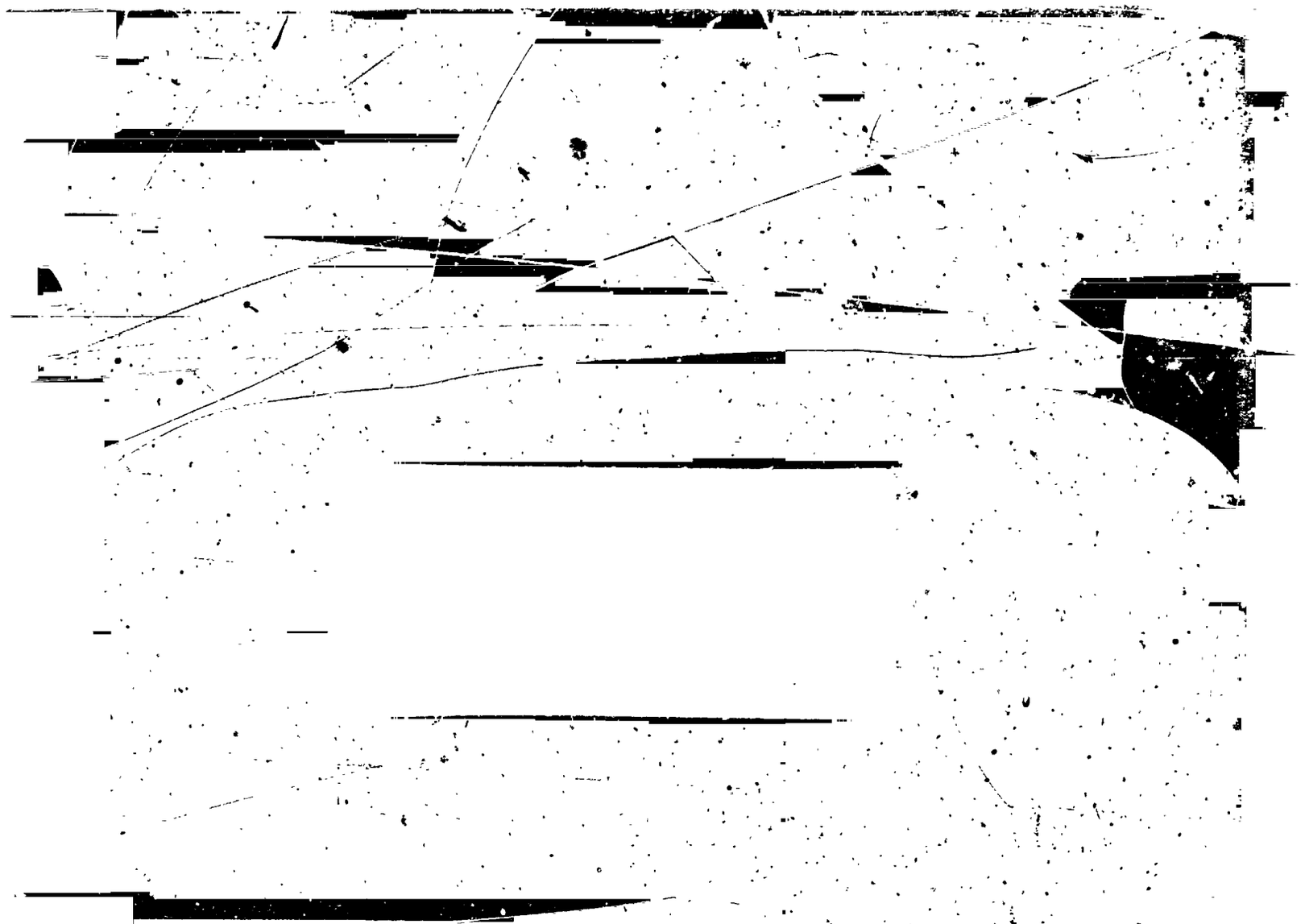

GPO PRICE $ _____

CFSTI PRICE(S) $ _____

Hard copy (HC) 2.00

Microfiche (MF) .50

ff 653 July 65

WT 20-499

RESULTS OF THE JPL AERODYNAMIC DAMPING-IN-PITCH WIND-TUNNEL PROGRAM

Duane A. Nelson

Robert E. Covey

Robert E. Covey, *Chief*
Aerodynamic Facilities Section

Copy No. 5

under NAS 7-100

JET PROPULSION LABORATORY
CALIFORNIA INSTITUTE OF TECHNOLOGY
PASADENA, CALIFORNIA
November 2, 1962

CONTENTS

FIGURES

PLOTS

Plot No.	Mach No.	Model	q (psia)
1	1.8	A-5a	0.9
↓	↓	↓	1.5
↓	↓	↓	3.0
2	3.3	↓	0.4
↓	↓	↓	0.8
↓	↓	↓	1.5
↓	↓	↓	3.0
3	4.0	↓	1.5
4	5.1	↓	0.3
↓	5.0	↓	1.5
↓	5.1	↓	2.0
↓	5.1	↓	2.8
5	6.0	↓	1.7
6	1.8	C.S.*	1.0
↓	↓	↓	1.6
↓	↓	↓	3.2
7	3.3	↓	0.4
↓	↓	↓	1.6
↓	↓	↓	3.2
8	4.0	↓	1.6

PLOTS (Cont'd)

Plot No.	Mach No.	Model	q (psia)
8	6.1	C.S.*	1.5
9	5.0	↓	0.4
↓	5.0	↓	1.6
↓	5.1	↓	2.7
10	6.0	A-2	0.2
↓	↓	A-5	↓
↓	↓	B-2a	↓
↓	↓	A-1	↓
11	6.0	B-2a	↓
↓	6.0	↓	0.5
↓	8.3	↓	0.4
12	6.0	A-1	0.2
↓	6.0	↓	0.5
↓	6.1	↓	1.0
13	6.0	A-2	0.2
↓	↓	A-2	0.5
↓	↓	B-2	↓
14	↓	B-2a	↓
14	↓	B-2	↓
15	↓	A-2	0.2

PLOTS (Cont'd)

Plot No.	Mach No.	Model	q (psia)
15	4.5	A-2	0.4
15	3.0	A-2	0.3
16	6.0	C.S.*	0.7
↓	6.1	↓	0.9
↓	6.0	↓	0.2
17	3.3	A-5a	3.0
18	↓	↓	↓
19	↓	↓	↓
20	↓	C.S.*	3.2
21	↓	↓	↓
22	↓	↓	↓
23	1.8	A-5a	3.0
24	↓	↓	↓
25	↓	↓	↓
26	6.0	↓	1.7
27	6.0	↓	1.7
28	6.1	C.S.*	2.9
29	↓	↓	↓
30	↓	↓	↓
31	↓	↓	2.6

PLOTS (Cont'd)

Plot No.	Mach No.	Model	q (psia)
32	6.1	C.S.*	2.6
33	6.1	C.S.*	2.6
34	2.0	A-2	2.6
34	3.0	A-2	2.7

*C.S. means "calibration sphere".

I. INTRODUCTION

This Report presents the results of Wind-tunnel Tests 20-465, 20-499C, 21-88, 21-106A, and 21-106B, which were tests of the JPL dynamic stability models. The purpose of the tests was to obtain aerodynamic damping-in-pitch data. The approximate aerodynamic parameters for the tests* were Mach No. 1.81, 2.01, 3.01, 3.26, 3.99, 4.54, 5.0, 6.0, and 8.3, and Reynolds No. from 0.01×10^6 to 0.30×10^6/in.

The model configurations consisted of a sphere, a truncated cone with spherical ends, a truncated cone with spherical front end and conical rear end, and a truncated cone with spherical front end and flat rear end. Data were obtained using an electronic angle-of-attack readout system on Tests 20-465, 20-484, and 21-88, and photographic data were taken on the other tests using a 16-mm motion-picture camera at 64, 128, and 200 frames/sec.

These tests were run intermittently at the Jet Propulsion Laboratory (JPL) between October, 1961, and July, 1962.

II. MODEL DESCRIPTION

The models are shown in Fig. 1 and 2. A more detailed description of the models and components is contained in Ref. 1.

*The notations used in this Report are defined in the Nomenclature.

III. WIND TUNNEL AND INSTRUMENTATION

Reference 2 describes the design and operating characteristics of the 20-in. supersonic and the 21-in. hypersonic wind tunnels. The supersonic wind tunnel has a nominal test-section size of 20 in. square and a Mach range from 1.3 to 5.0. The hypersonic wind tunnel has a nominal test-section size of 21 in. square and a Mach range from 5 to 10. Both tunnels have flexible-plate nozzles and operate with continuous flow. Table 1 presents representative values of the test-section flow parameters for the Mach numbers at which these tests were conducted.

Reference 3 describes the electronic angle-of-attack readout device used in Tests 20-465, 20-484, and 21-80. On the remaining tests a 16-mm motion-picture camera was used to photograph (1) the model motion, and (2) a mechanical time counter.

IV. TEST PROCEDURE

Prior to actual test operations, all models (except the calibration sphere) were statically balanced about their respective defined centers of gravity. Since, during the test, the models were to be mounted on a gas bearing (using gaseous nitrogen as its lubricant), the damping due to the bearing had to be measured. This measurement was made by (1) allowing a sphere (calibration sphere) containing an off-center weight to oscillate in the wind-tunnel air flow, and (2) recording the angle-of-attack vs time history. Then, each of the other models, mounted in turn on the gas bearing, was pitched to its maximum

angle-of-attack, released, and allowed to oscillate until damped by the air flow and the bearing friction.

V. DATA REDUCTION

The coefficients $\left(C_{m_q} + C_{m_{\dot{\alpha}}}\right)$/rad/sec were calculated assuming that the coefficients of the governing equation of motion

$$I\ddot{\alpha} + M_D\dot{\alpha} + \left(\frac{C_m qSd}{\alpha}\right)\alpha = 0 \tag{1}$$

are constant for each cycle of oscillation. The solution of this linear differential equation yields

$$M_D = -2If \log_e \left(1 - \frac{\Delta\alpha}{\alpha}\right) \tag{2}$$

The dynamic stability coefficient is defined as

$$\left(C_{m_q} + C_{m_{\dot{\alpha}}}\right)/\text{rad/sec} = \frac{VM_D}{qSd^2} \tag{3}$$

Reference 3 describes in more detail the data reduction for Tests 20-484 and 21-88. For the remaining tests, however, the maximum angular excursion on every tenth cycle of oscillation and the elapsed time for that maximum excursion were read directly from the motion-picture film.

The average frequency, f, over ten cycles of oscillation is computed from

$$f = \frac{10}{t_{(n+10)} - t_n} \tag{4}$$

The decay rate, $\Delta\alpha/\alpha$, is computed from

$$\frac{\Delta\alpha}{\alpha} = \frac{\alpha_n - \alpha_{(n+10)}}{\alpha_n} \tag{5}$$

VI. RESULTS

The results of this test have been reduced to coefficients, $\left(C_{m_q} + C_{m_{\dot{\alpha}}}\right)$/ rad/sec, and are presented in Plot Series 1 through 34. No attempt was made in this Report to interpret the results.

The repeatability of $\left(C_{m_q} + C_{m_{\dot{\alpha}}}\right)$/rad/sec for all Mach numbers is ±0.005 for the models, and about ±0.001 for the calibrating sphere.

The plotted data presented in this Report have been corrected for bearing friction; i.e., the calibration-sphere damping has been subtracted from the corresponding model damping data. Some of the sphere data presented in the Plots have been taken from two "contractor" tests (Tests 20-516 and 21-113).

Plots 17 through 33 contain angle-of-attack vs time history for complete cycles of model oscillation. There are usually three plots per run in order to obtain data at the beginning, middle, and end of each run.

Plot 34 presents the data obtained using a ball bearing rather than the gas bearing. The damping of the ball bearing could not be measured experimentally, so an empirical equation was used to estimate the bearing damping to an accuracy of about ± 50%.

NOMENCLATURE

Data Reduction

C_m	local pitching-moment coefficient
$\left(C_{m_q} + C_{m_{\dot{\alpha}}}\right)$	aerodynamic damping in pitch coefficient (per radian per second) taken to be the average damping in any given cycle
d	maximum model diameter = 4.000 in. for the A-1, A-2, A-5, B-2, B-2a, and C.S.; 3.600 in. for the A-5a
f	frequency of model oscillation (cycles/sec)
I	measured moment of inertia about the model axis of rotation of the model and the gas bearing
M	Mach number
m_d	damping moment (in.-lb-sec)
n	subscript; refers to the condition occurring on the n^{th} cycle of model oscillation
(n+10)	subscript; refers to the conditions occurring during the tenth cycle after the n^{th} cycle
P	static pressure in the wind tunnel (psia)
P_t	wind-tunnel stagnation pressure (psia)
q	wind-tunnel dynamic pressure (psia)
Re	Reynolds number per inch
S	model frontal area = 12.566 $in.^2$ for the A-1, A-2, A-5, B-2, B-2a, and C.S.; 10.179 $in.^2$ for the A-5a
V	free-stream wind-tunnel velocity (in./sec)
α	model angle of attack referenced to the wind-tunnel centerline (deg)
$\dot{\alpha}$	model angular velocity (rad/sec)
$\ddot{\alpha}$	model angular acceleration (rad/sec^2)
$\Delta\alpha$	$\alpha_n - \alpha_{(n+10)}$

REFERENCES

1. JPL Drawing No. 4-9133079, Aft Body--Dynamic Stability A-5 Shape; 5-9133148, Gas-Bearing Sting Mount; 5-9133159, Models--Sting Mount; 6-9132813, Models--Mariner (4-In. Dia. NASA Shape); 6-9132819, Models--Mariner (4-In. Dia. JPL Shape); 6-9132834, Models--Mariner (Installation and Assembly); 6-9133081, Model--Mariner (4-In. Dia. Sphere); 6-9133173, Air Bearing Installation--Sting Mount. UNCLASSIFIED.

2. Jet Propulsion Laboratory, California Institute of Technology. Wind-Tunnel Facilities at the Jet Propulsion Laboratory. Pasadena, California, JPL, April 18, 1961. (Technical Release No. 34-257), UNCLASSIFIED.

3. Jet Propulsion Laboratory, California Institute of Technology. A Technique for Obtaining Dynamic Stability Derivatives at Large Angular Amplitudes, by T. L. Babineaux, D. A. Nelson, and B. Dayman, Jr. Pasadena, California, JPL, April 16, 1962. (Internal Memorandum JPL WT G-T15), UNCLASSIFIED.

Table 1. Average aerodynamic parameters

Parameter	Mach Number							
	1.81	3.01	3.26	3.99	4.54	5.0	6.0	8.27
Static pressure (psia)	0.819	0.052	0.208	0.140	0.025	0.096	0.026	0.009
Stagnation pressure (psia)	4.78	1.93	11.25	20.90	7.70	50.36	40.45	108.43
Dynamic pressure (psia)	1.78	0.33	1.55	1.55	0.37	1.69	0.65	0.43
Reynolds number (per in. x 10^{-6})	0.110	0.024	0.120	0.151	0.046	0.127	0.080	0.021

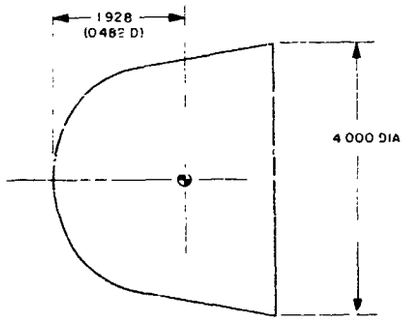

A-1

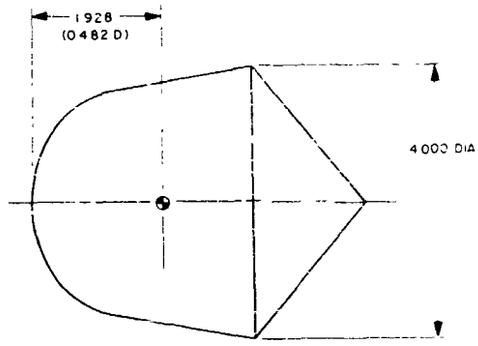

A-2

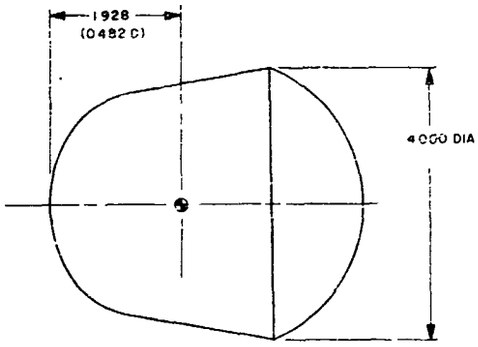

A-5

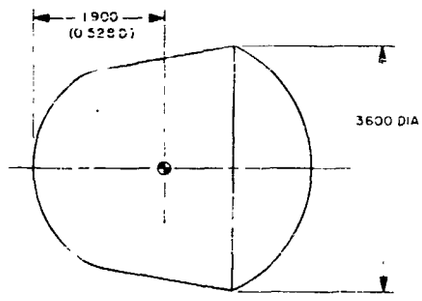

A-5a

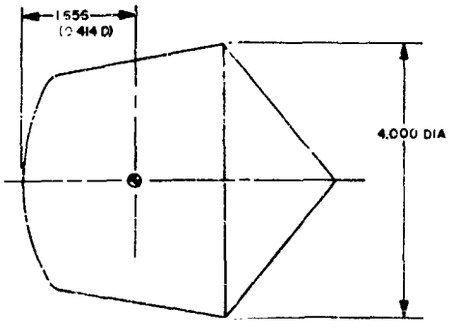

B-2

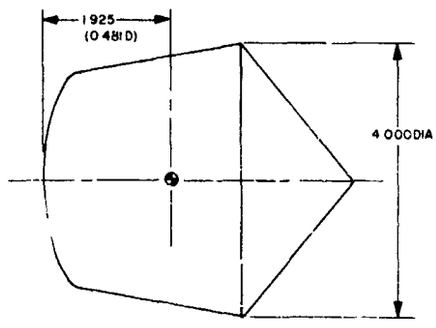

B-2a

Fig. 1. Model Configurations

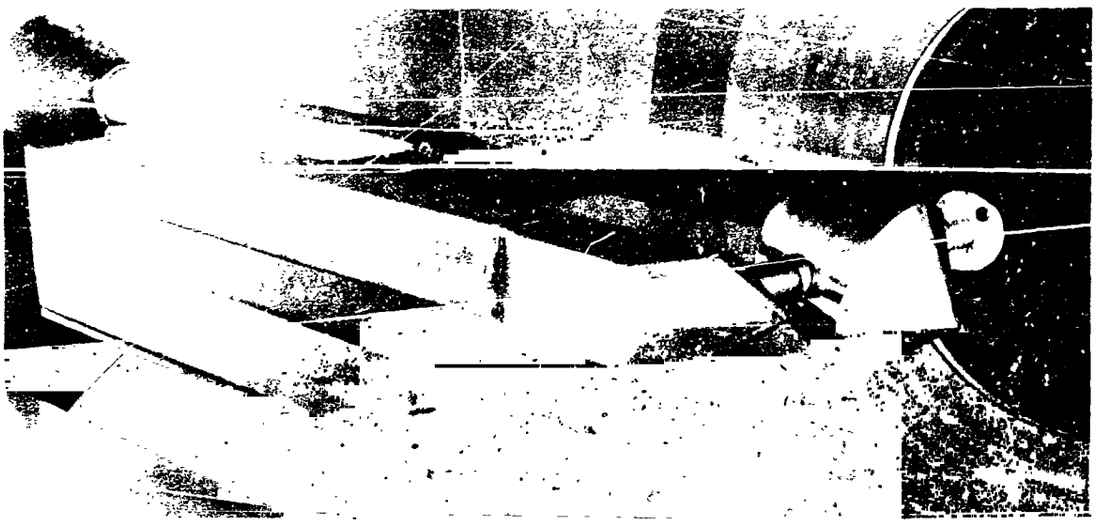

Model A-2 installed in the 21-in. tunnel on the cross-strut support that was used in tests 20-484 and 21-88

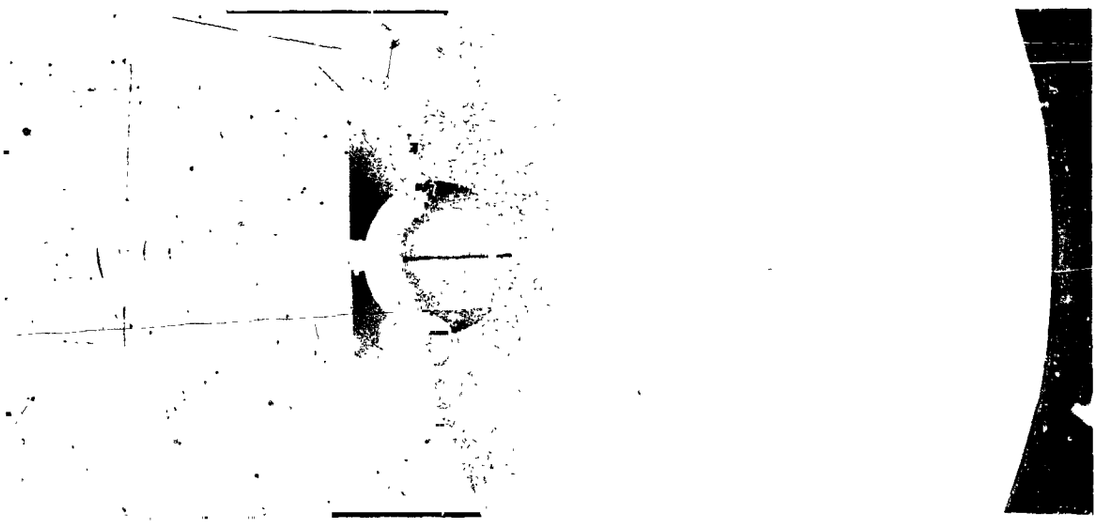

Calibrating sphere installed in the 20-in. tunnel on the sting mount that was used in tests 20-499C, 21-106A, and 21-106B

Fig. 2. Models Installed in the Wind Tunnel Test Section

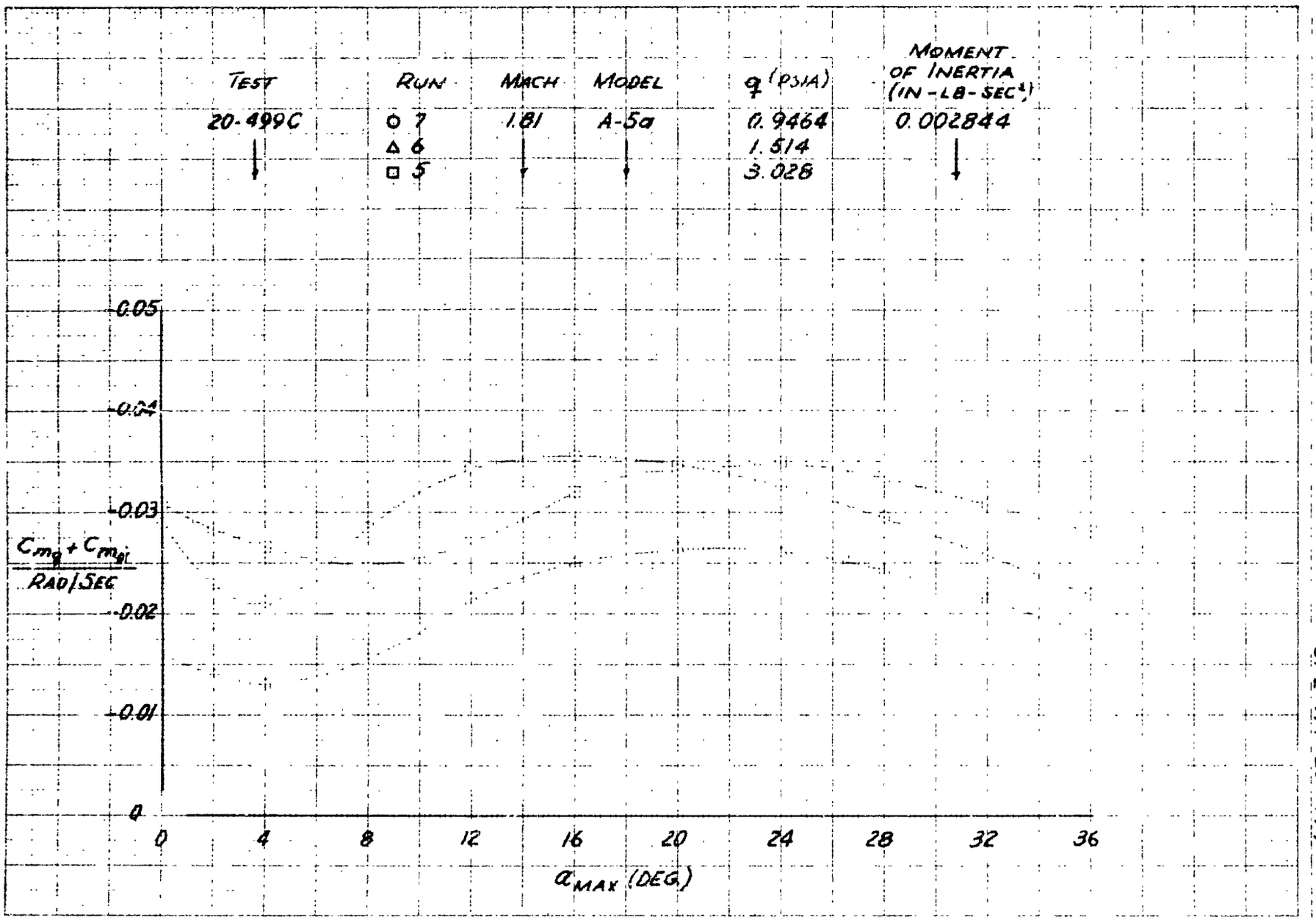

PLOT 1

JPL WT 20-499

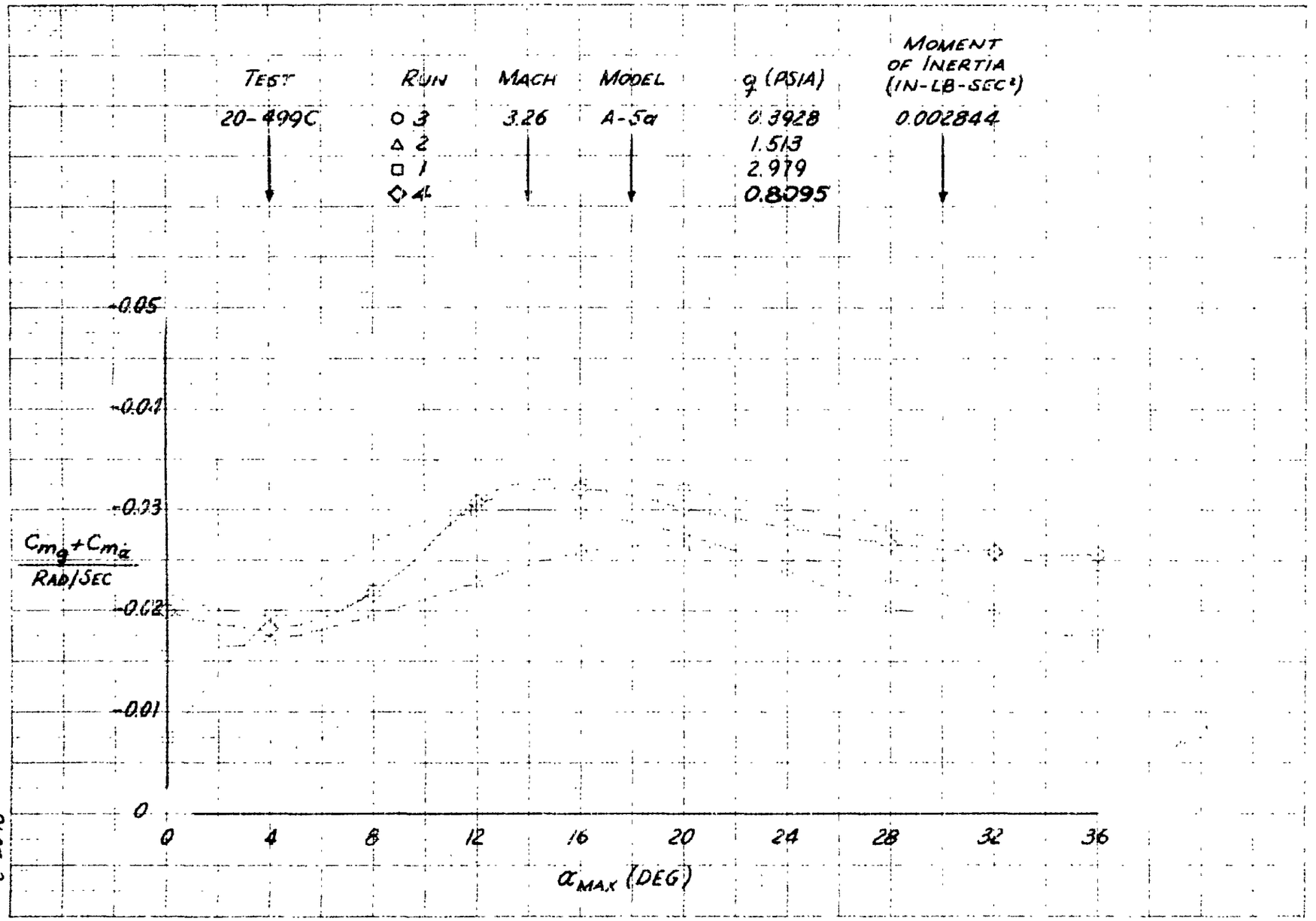

PLOT 2.

CAL WT 20-499

TEST	RUN	MACH	MODEL	q (PSIA)	MOMENT OF INERTIA (IN-LB-SEC^2)
20-499C	011	3.99	A-5α	1.519	0.002844

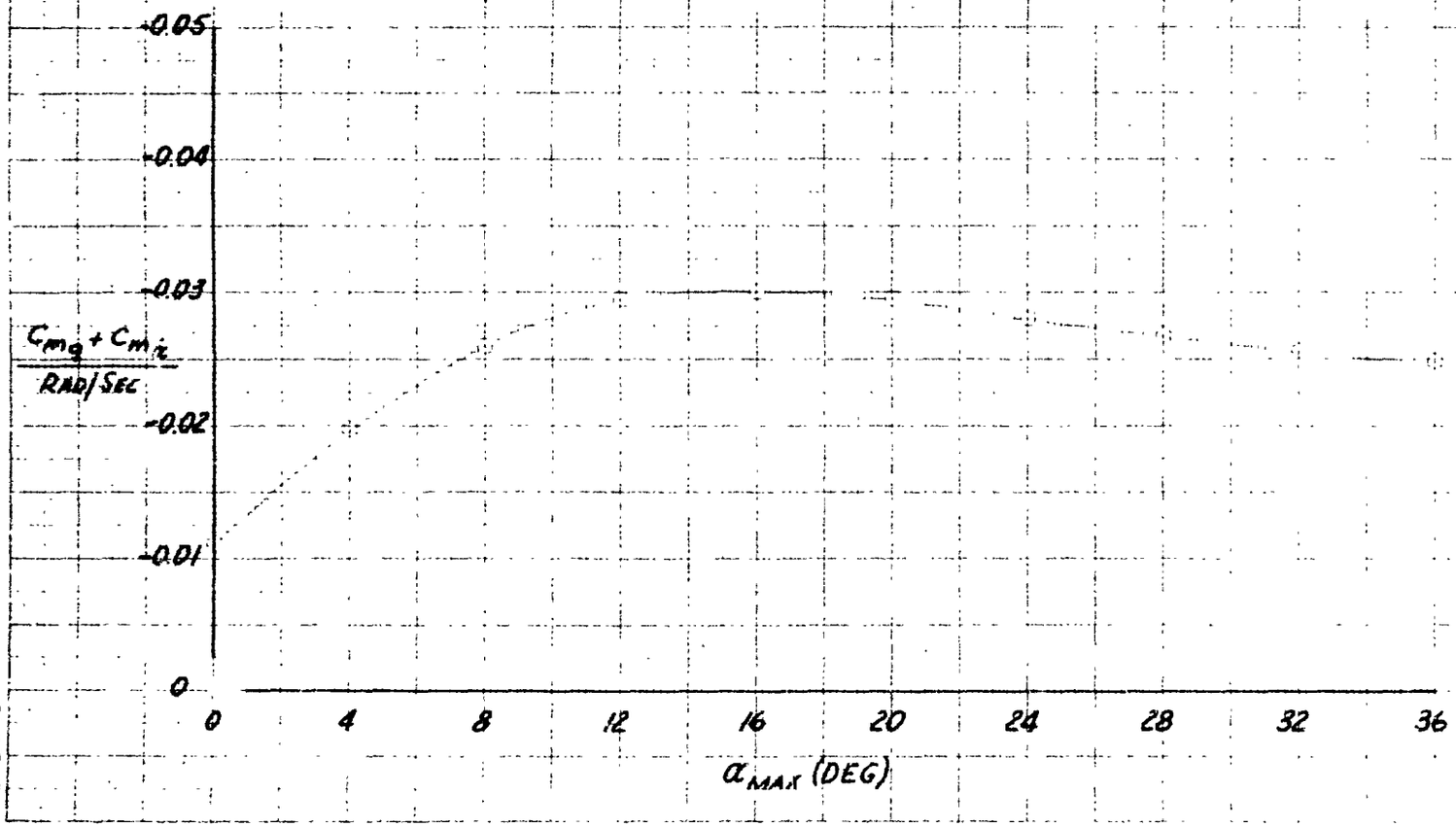

JPL WT 20-499

PLATE 4

TEST	RUN	MACH	MODEL	q (PSIA)	MOMENT OF INERTIA (IN-LB-SEC²)
21-106B	○ 28	5.13	A-5α	0.306	0.002844
	△ 27	5.04		1.458	
	□ 25	5.07		1.993	
	◇ 26	5.08		2.829	

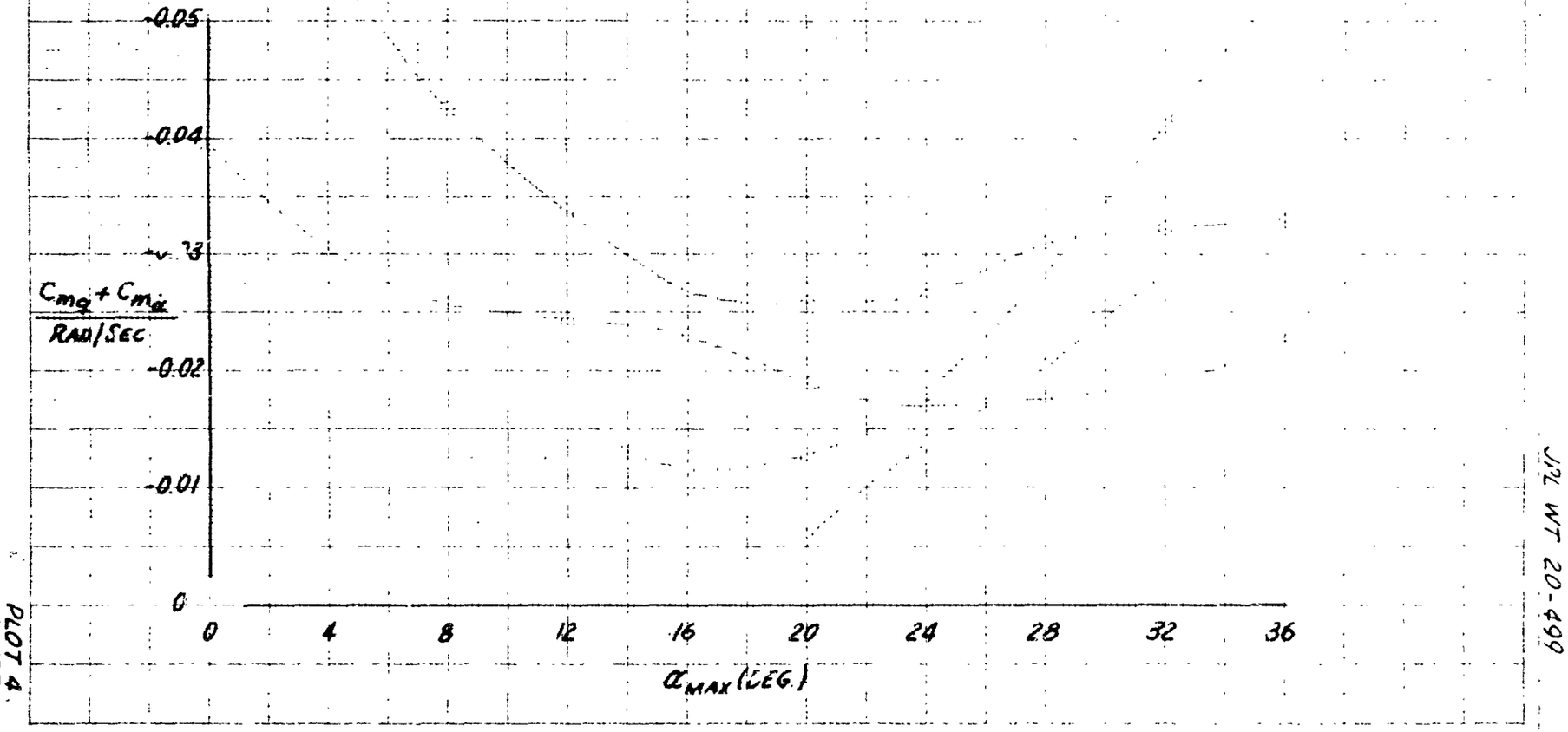

PLOT 4

UPL WT 20-499

TEST	RUN	MACH	MODEL	q (PSIA)	MOMENT OF INERTIA (IN-LB-SEC²)
21-106A	03	5.95	A-5α	1.685	0.002844

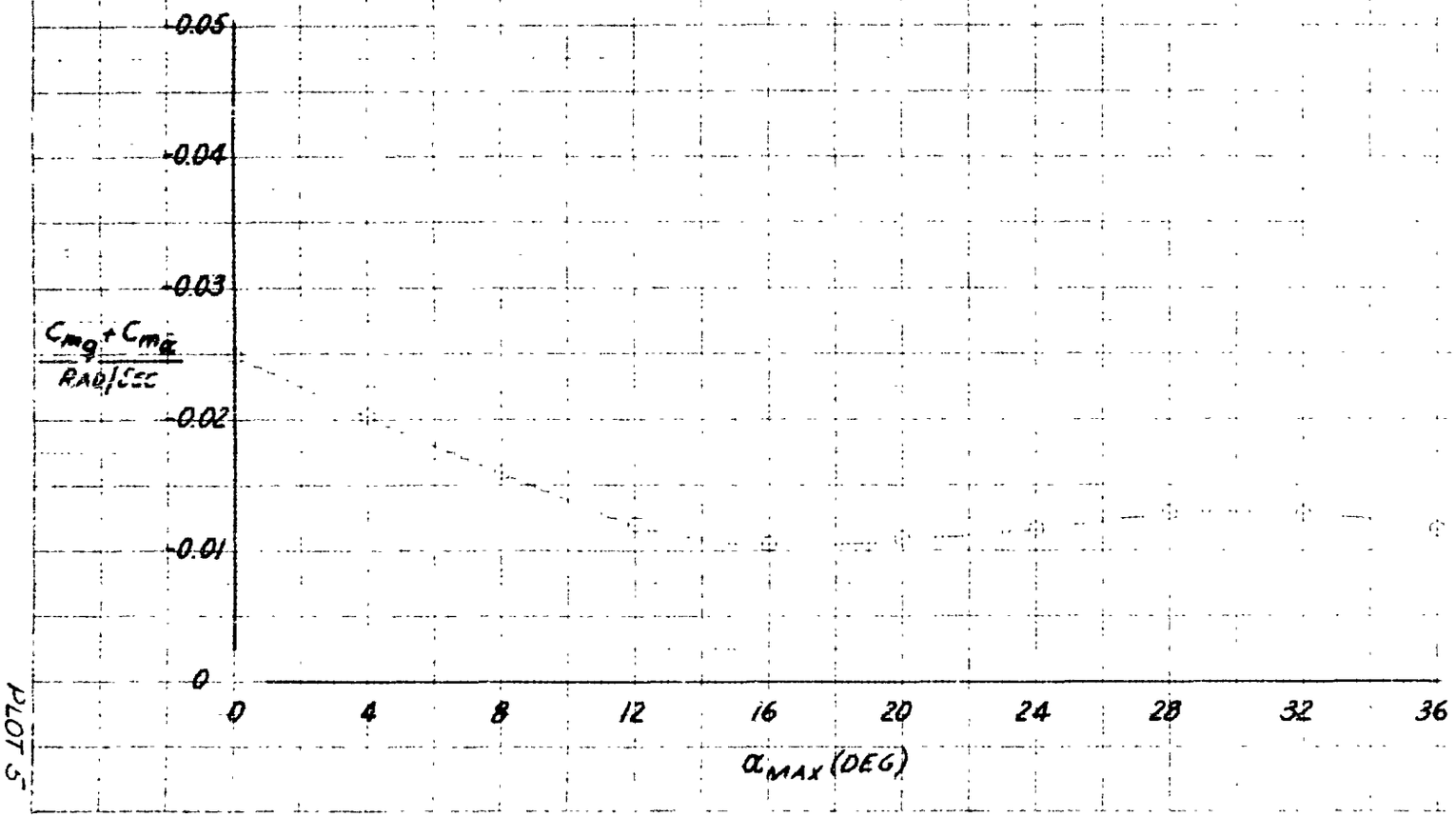

PLOT 5

JPL WT 20-499

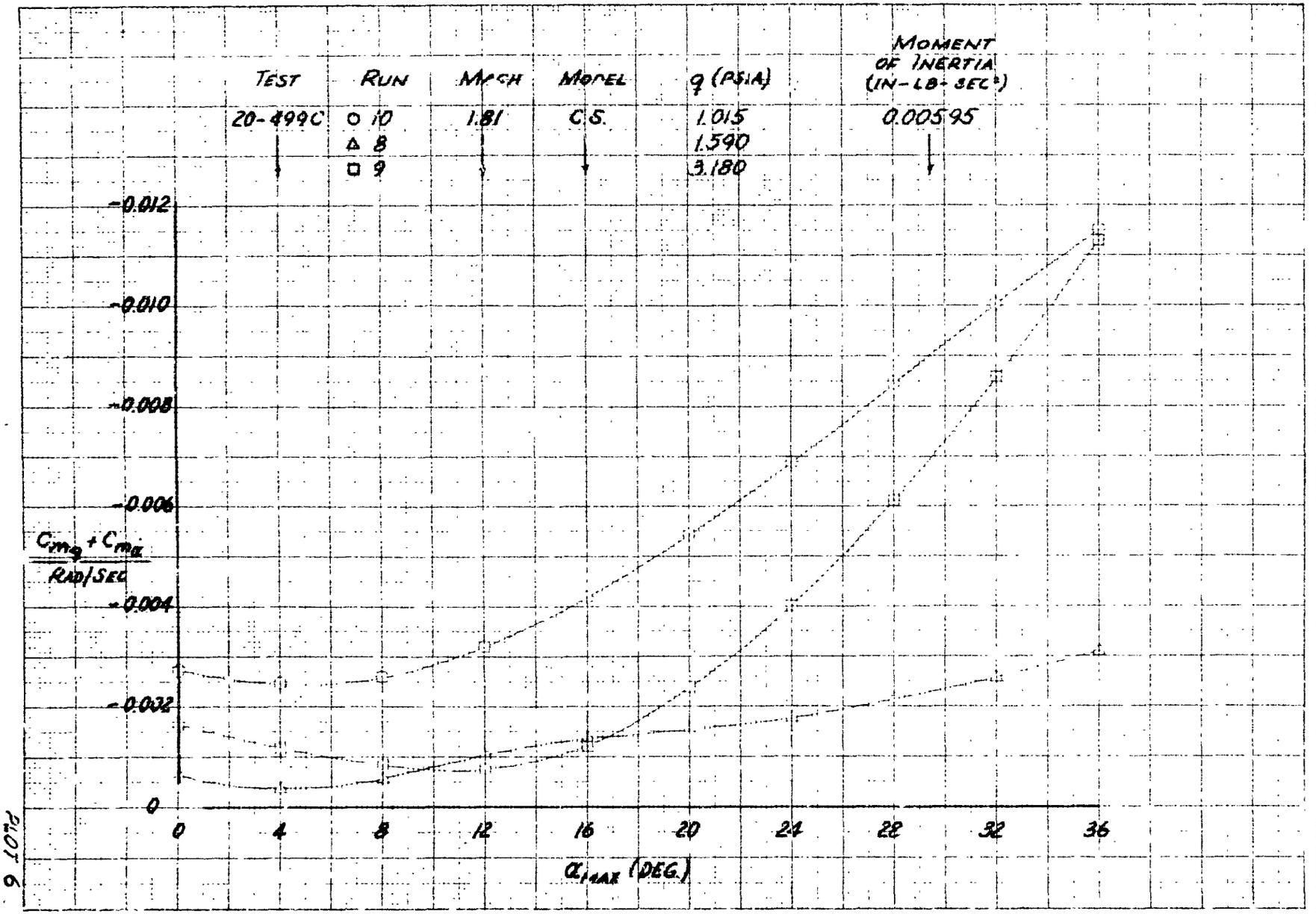

PLOT 6

JPL W.T. 20-495

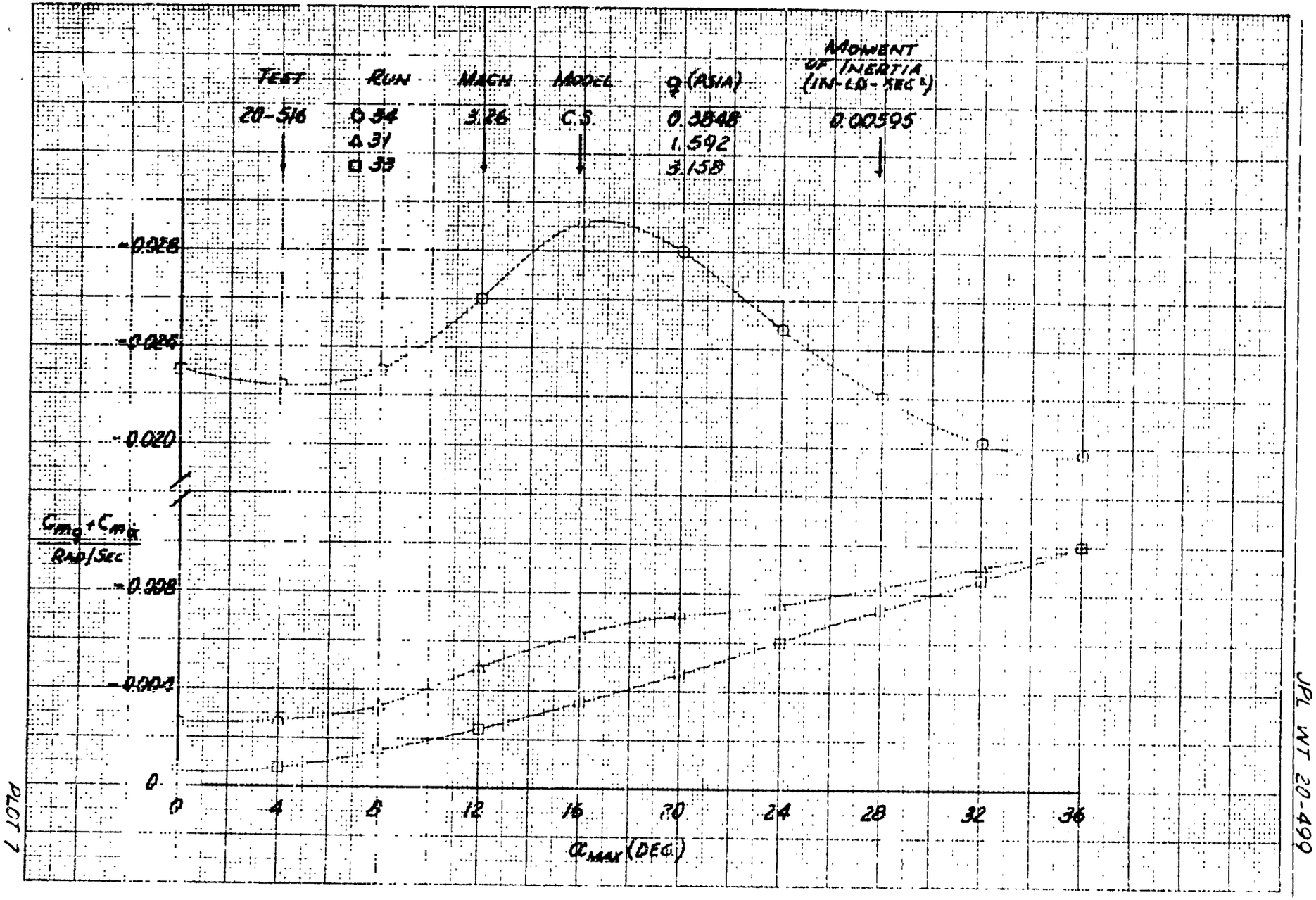

PLOT 1

JPL WT 20-490

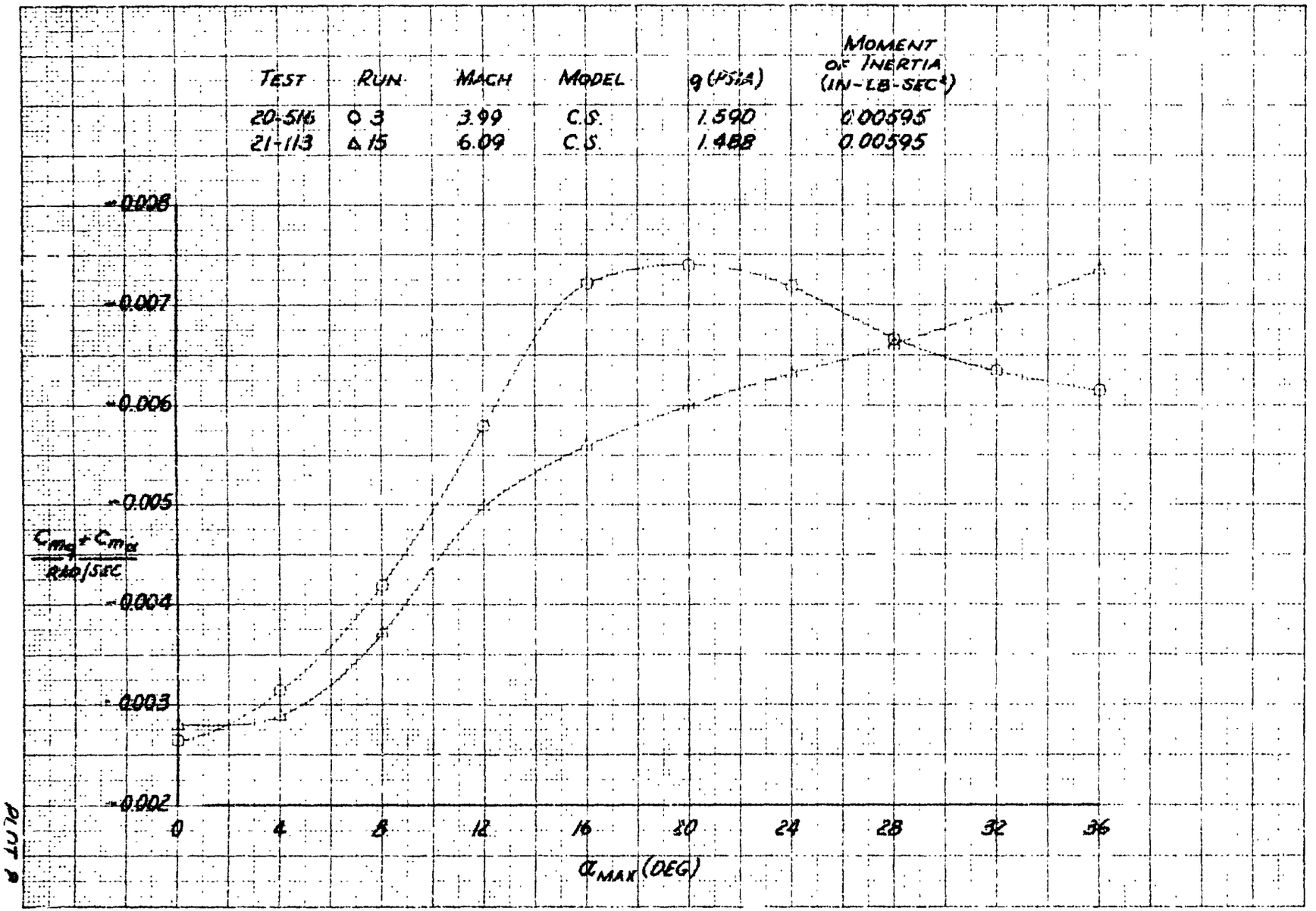
TEST
RUN
MACH
MODEL
q (PSIA)
MOMENT OF INERTIA (IN-LB-SEC²)
20-516
0 3
3.99
C.S.
1.590
0.00595
21-113
Δ 15
6.09
C.S.
1.488
0.00595
-0.008
-0.007
-0.006
-0.005
-0.004
-0.003
-0.002
$\frac{C_{m_q} + C_{m_{\dot{\alpha}}}}{RAD/SEC}$
0
4
8
12
16
20
24
28
32
36
α_{MAX} (DEG)

JPL WT 20-499

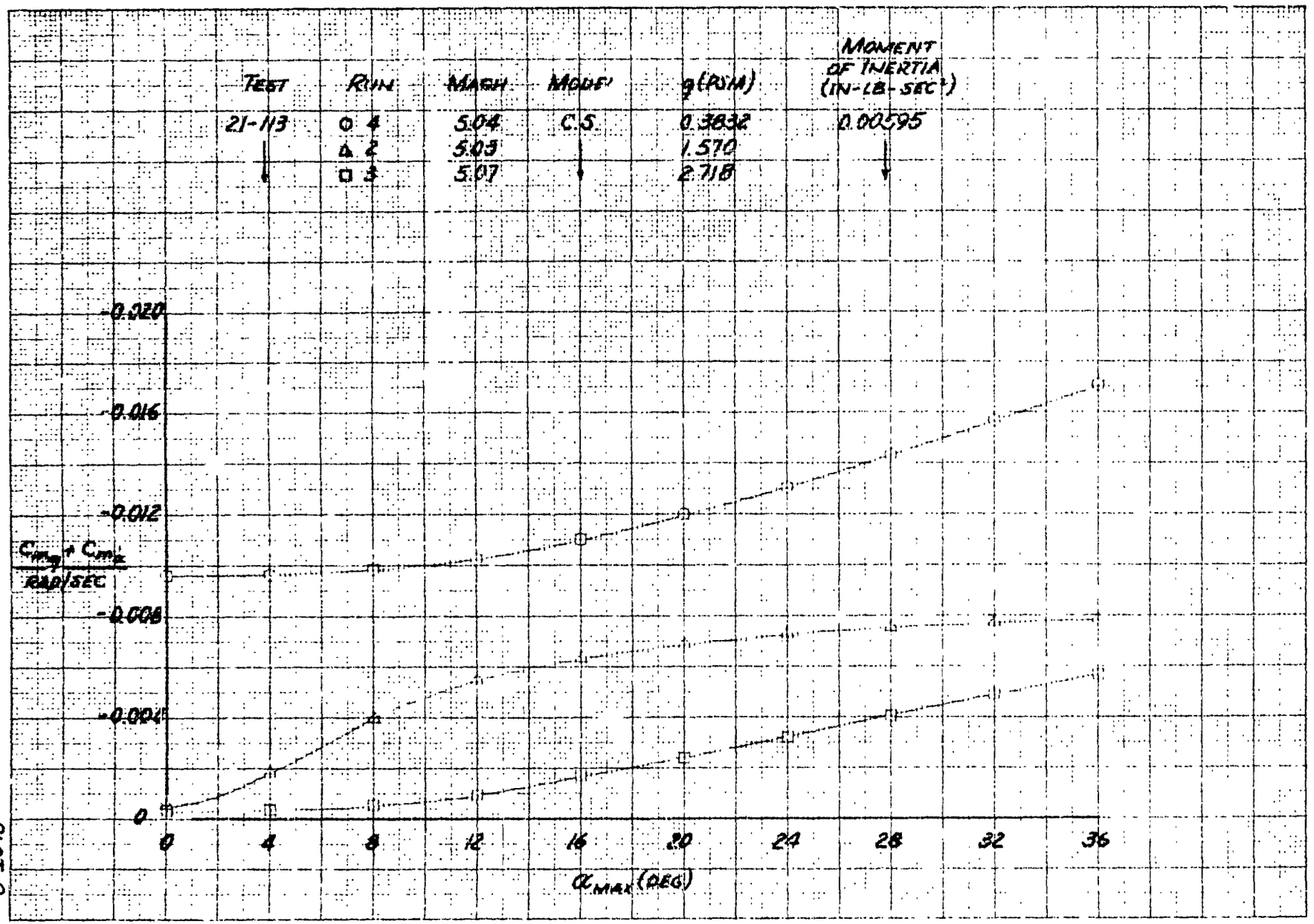

PLOT 9.

JPL WT 20-499

JPL WT 20-499

TEST	RUN	MACH	MODEL	$\bar{q}$ (PSIA)	MOMENT of INERTIA (IN-LB-SEC^2)
21-88	○ 16.1	5.95	A-2	0.239	0.01565
	△ 18.1		A-5		0.01631
	□ 19.1		B-2a	↓	0.01280
	◇ 6.2	↓	A-1	0.238	0.01420

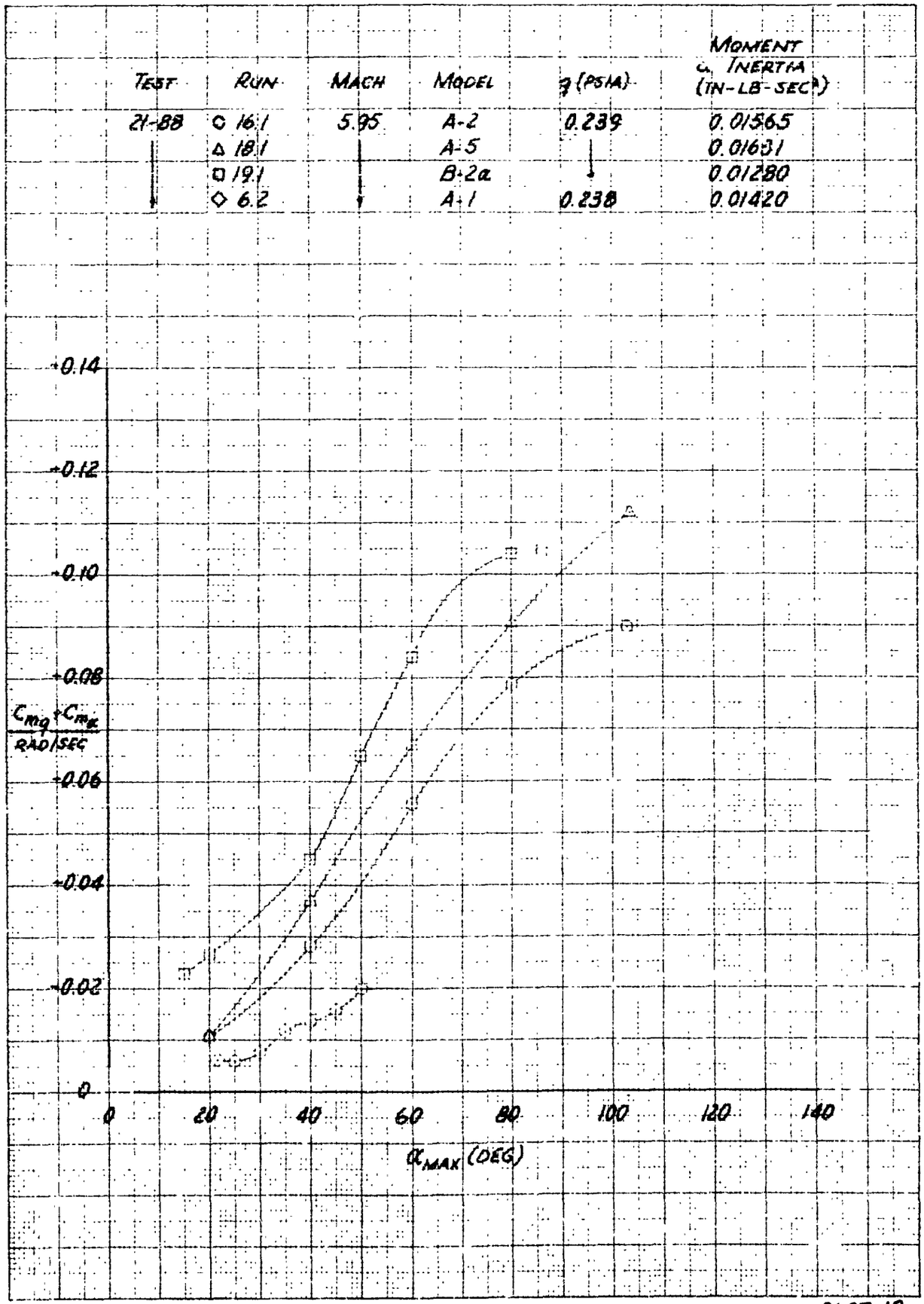

PLOT 10.

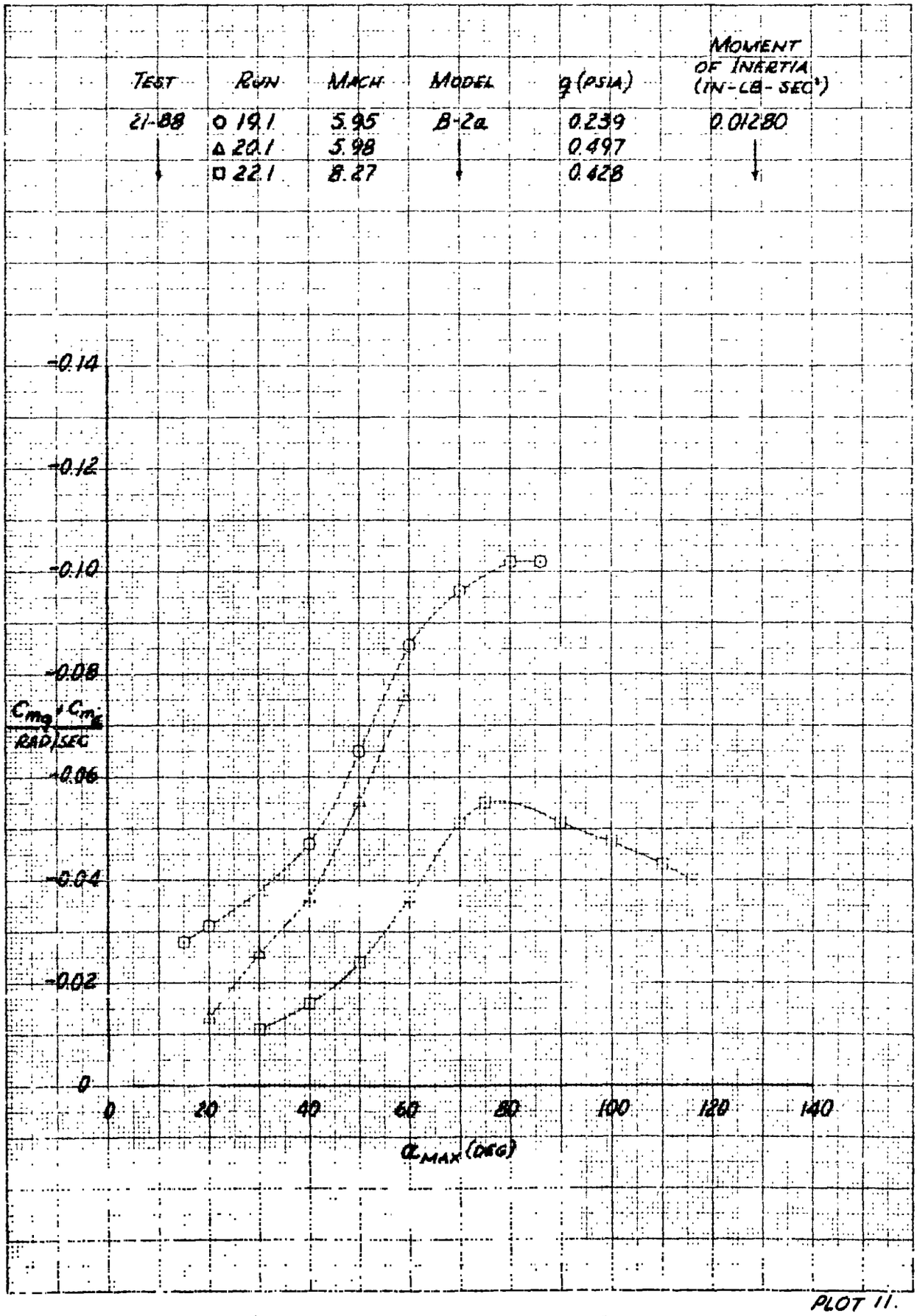
TEST
RUN
MACH
MODEL
q (PSIA)
MOMENT OF INERTIA (IN-LB-SEC²)
21-88
○ 19.1
△ 20.1
□ 22.1
5.95
5.98
8.27
B-2a
0.239
0.497
0.428
0.01280
-0.14
-0.12
-0.10
-0.08
-0.06
-0.04
-0.02
0
$C_{m_q} + C_{m_{\dot{\alpha}}}$ / RAD/SEC
0
20
40
60
80
100
120
140
α_{MAX} (DEG)

PLOT 11.

JPL WT 20-499

TEST	RUN	MACH	MODEL	q (PSIA)	MOMENT OF INERTIA (IN-LB SEC^2)
21-88	○ 6.2	5.95	A-1	0.238	0.01420
	△ 7.1	5.98		0.545	
	□ 7.1	6.05		1.040	

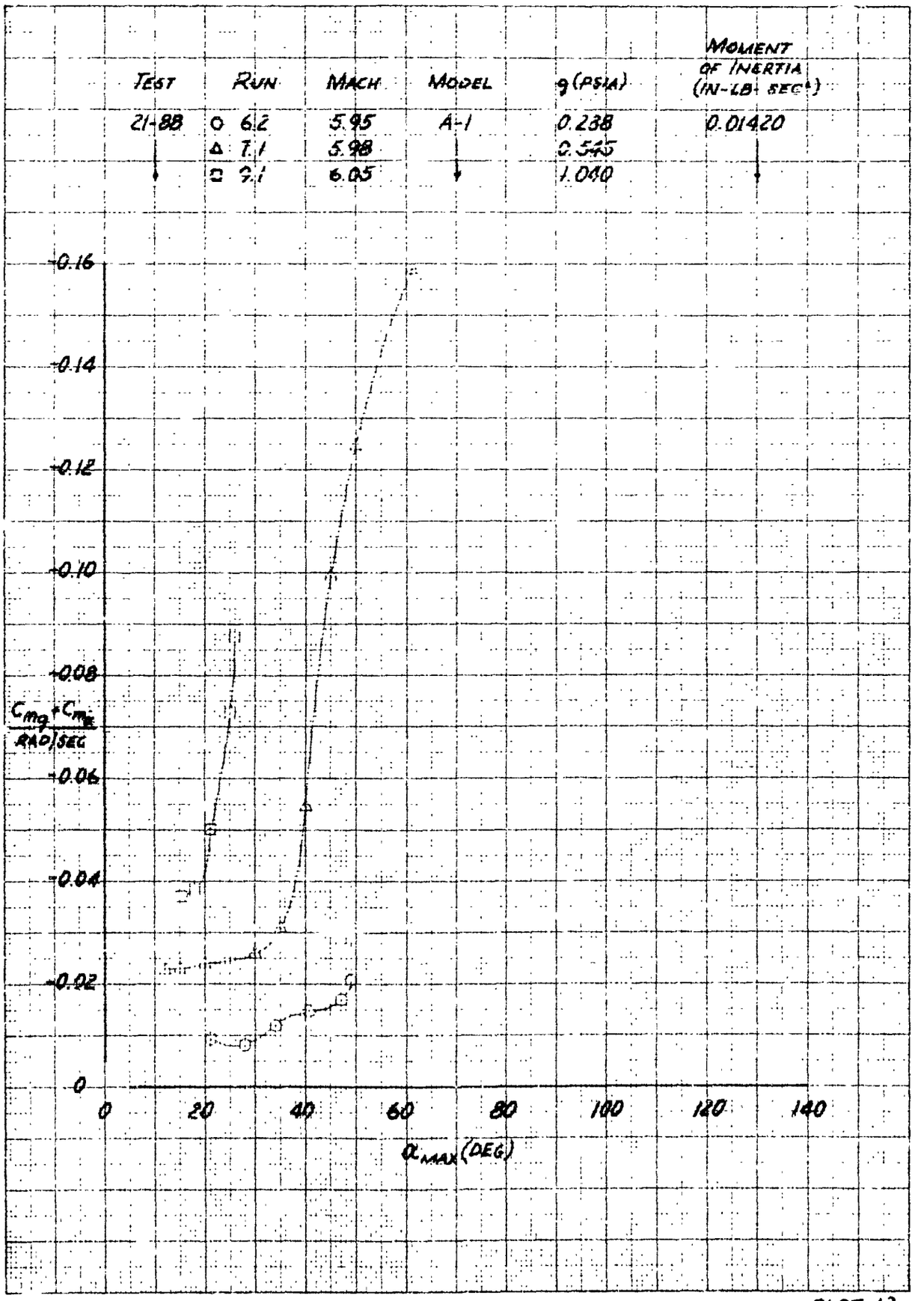

PLOT 12.

TEST	RUN	MACH	MODEL	q (PSIA)	MOMENT OF INERTIA (IN-LB-SEC^2)
21-68	○ 16.1	5.95	A-2	0.239	0.01565
	△ 17.1	5.98	A-2	0.499	0.01565
↓	□ 21.1	5.98	B-2	0.499	0.01280

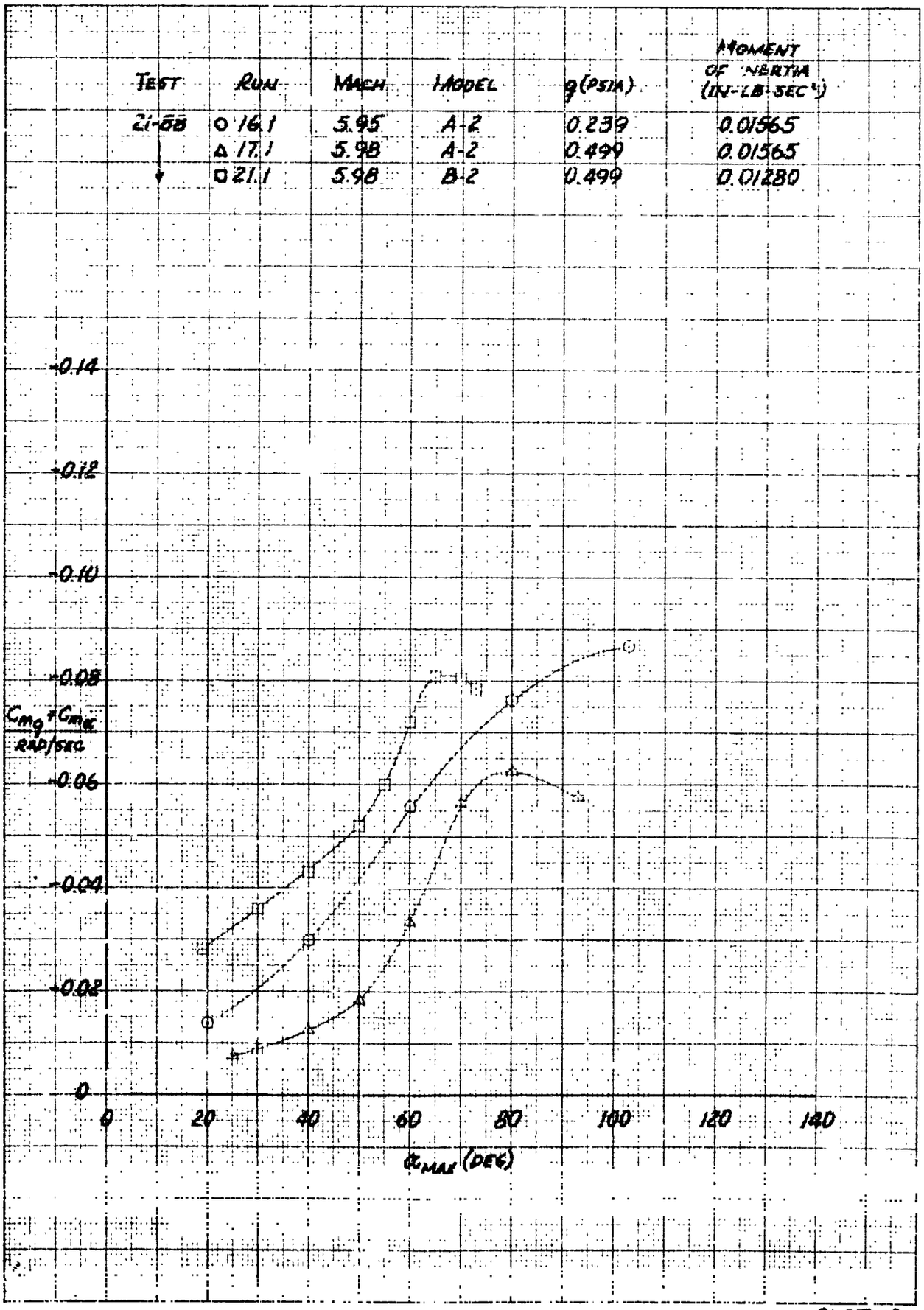

PLOT 13.

JPL WT 20-499

TEST	RUN	MACH	MODEL	q (PSIA)	MOMENT OF INERTIA (IN-LB-SEC^2)
21-88	○ 20.1	5.98	B-2a	0.491	0.01280
21-88	△ 21.1	5.98	B-2	0.499	0.01280

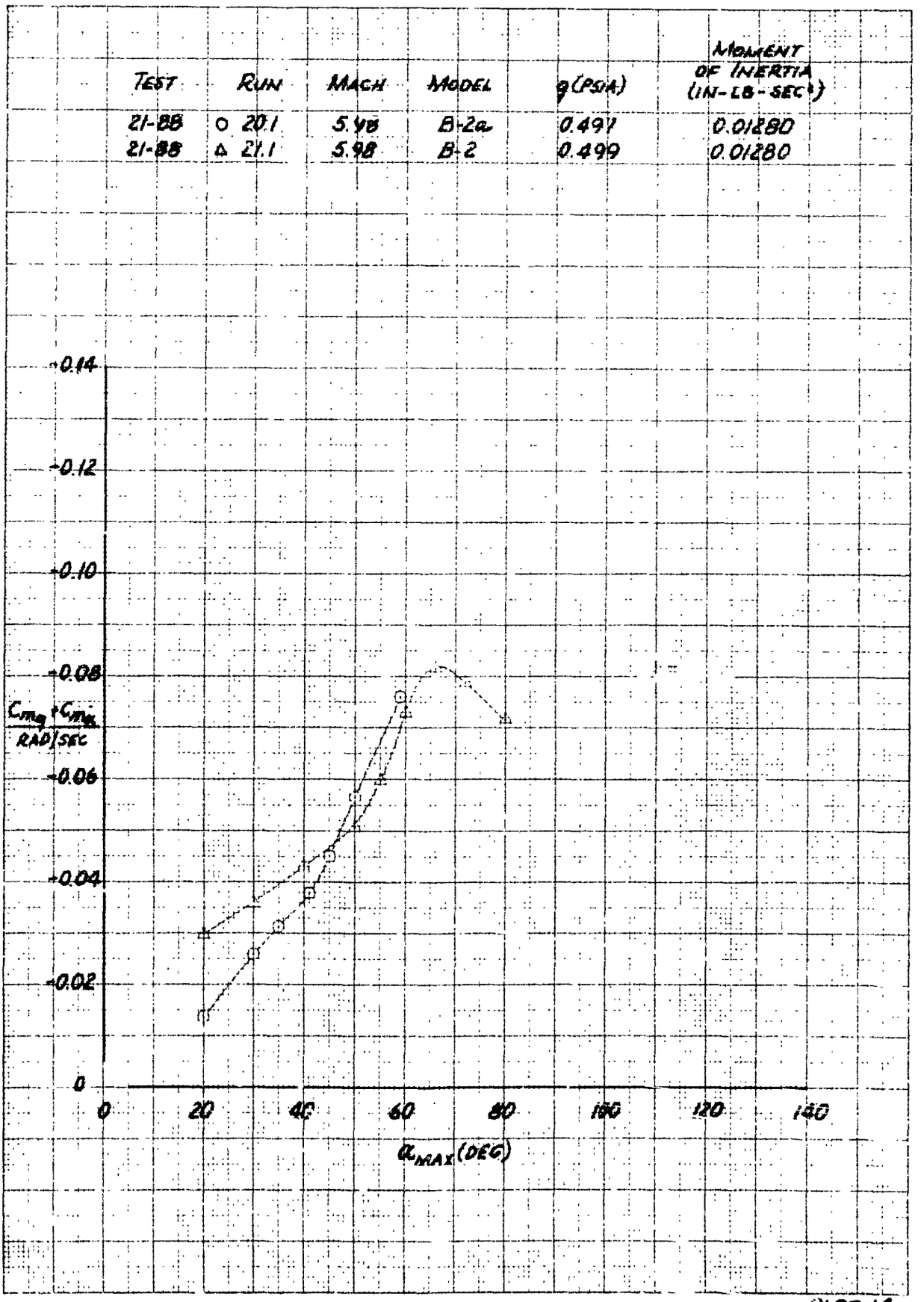

NOT 14.

JPL WT 20-499

TEST	RUN	MACH	MODEL	q (PSIA)	MOMENT OF INERTIA (IN-LB-SEC²)
21-88	○ 16.1	5.95	A-2	0.239	0.01565
20-484	△ 24.2	4.54	↓	0.365	↓
20-484	□ 37.1	3.01	↓	0.328	↓

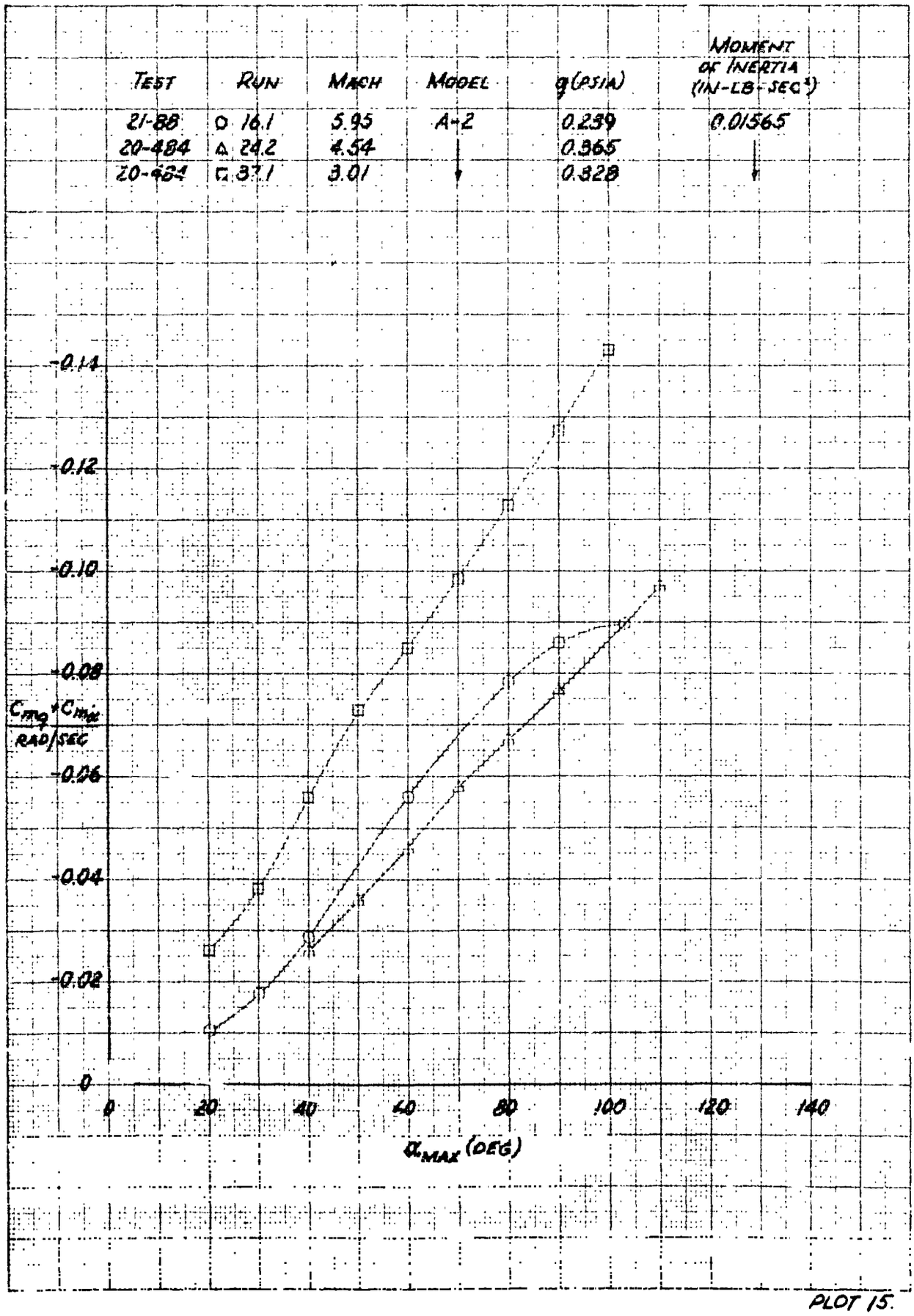

PLOT 15.

JPL WT 20-499

TEST	RUN	MACH	MODEL	q (PSIA)	MOMENT OF INERTIA (IN.-LB-SEC²)
21-88	○ 12.1	5.97	C.S.	0.675	0.00582
	△ 14.1	6.11		0.855	
	□ 15.1	5.95		0.239	

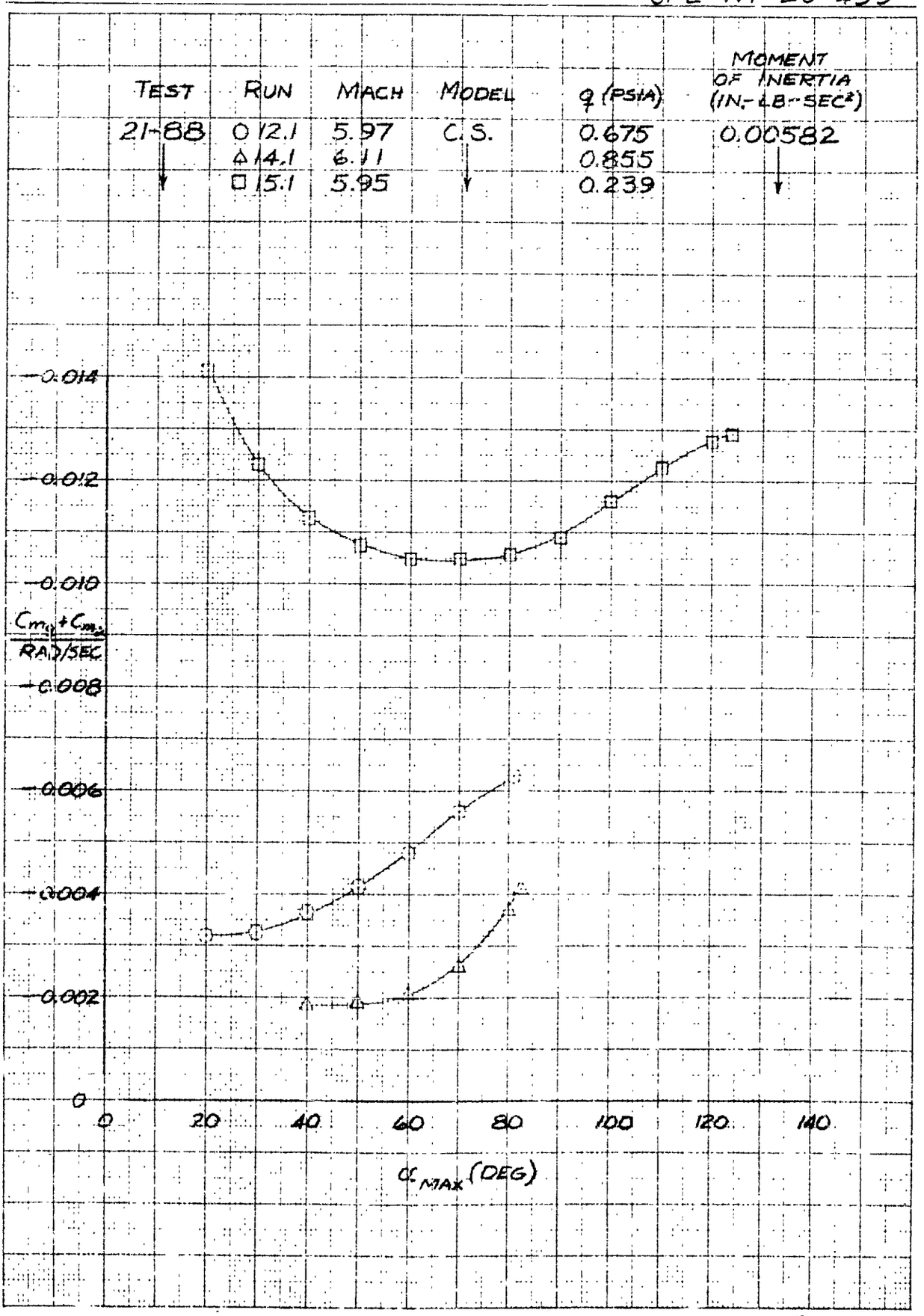

PLOT 16

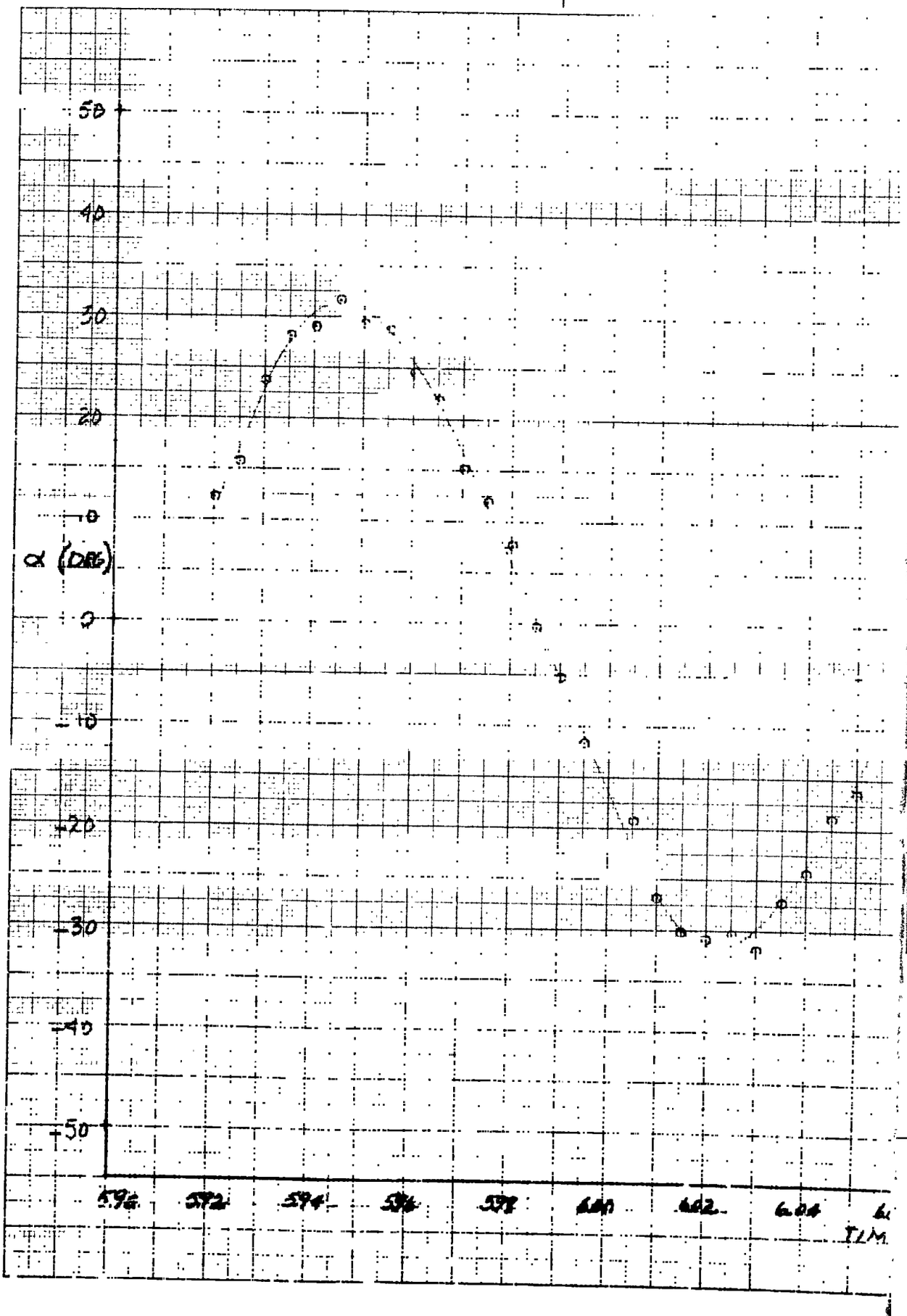
50
40
30
20
10
0
α (DEG)
-10
-20
-30
-40
-50
592
594
596
598
600
602
604
TIME

J

JPL WT 20-499

TEST: 2L-499C
MODEL: A-5a
MACH NO: 3.26
DYNAMIC PRESSURE: 2.999 PSI
RUN NO: 1
TIME: 6 sec.

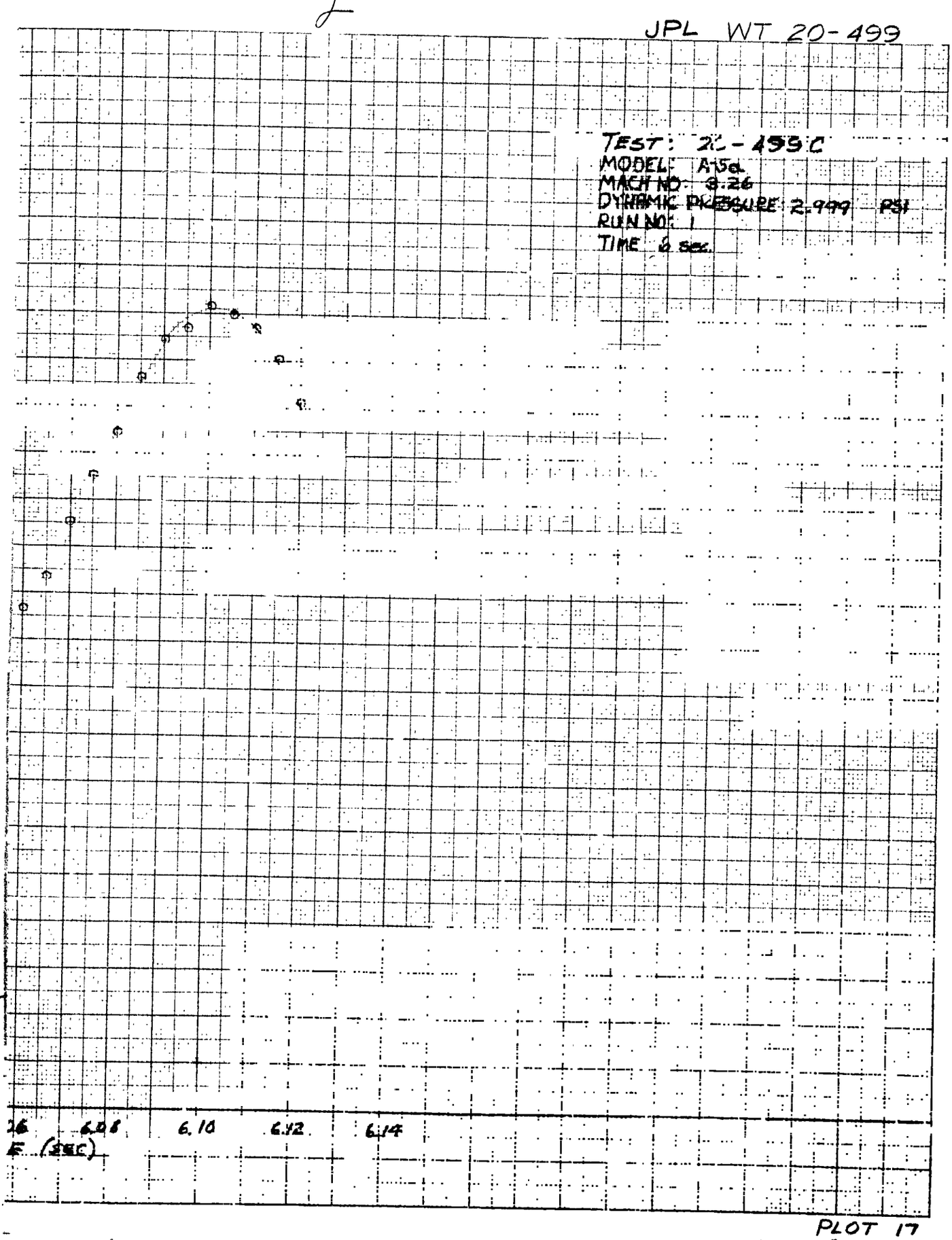

PLOT 17

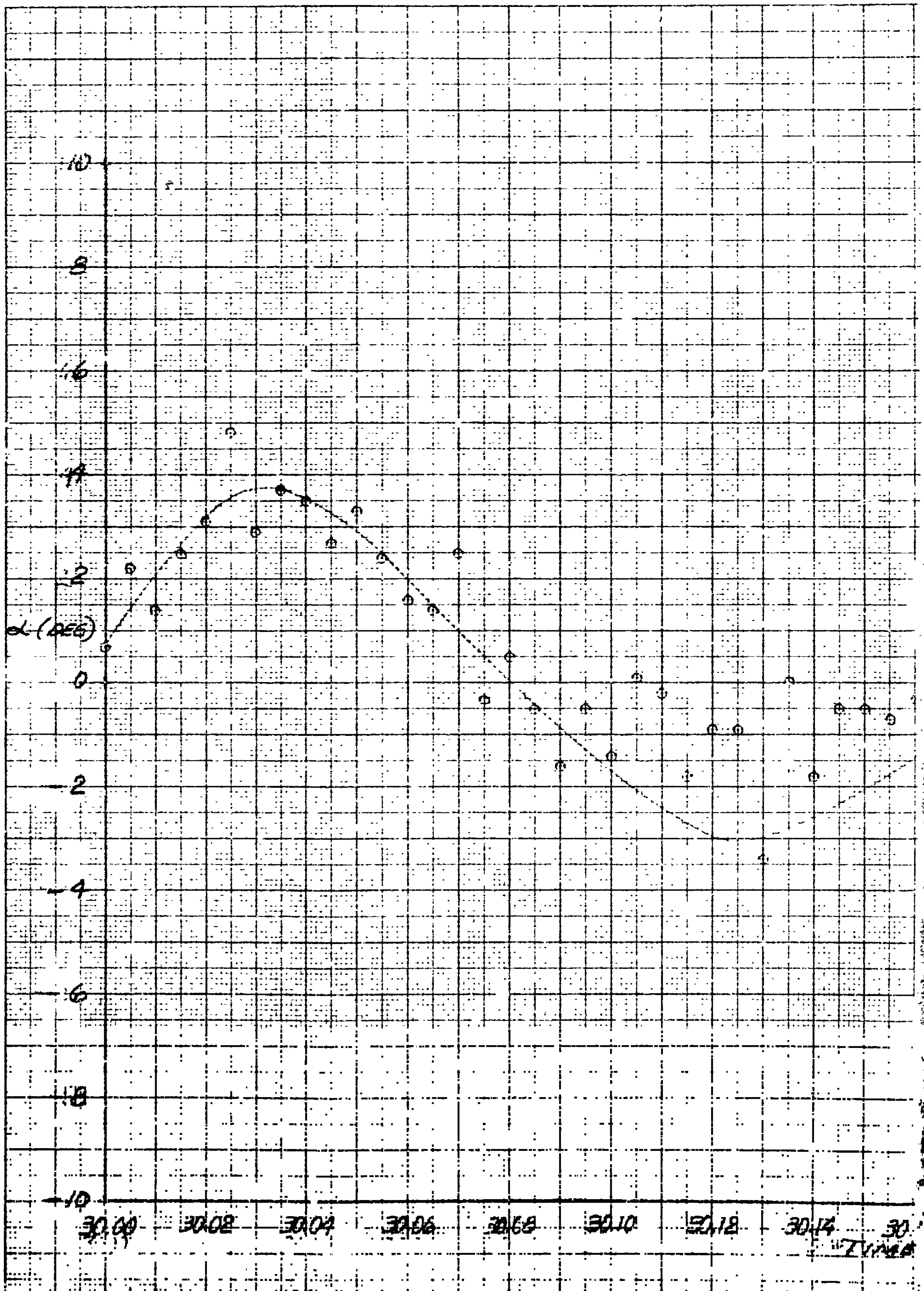
10
8
6
4
2
α (DEG)
0
-2
-4
-6
-8
-10
30.00
30.02
30.04
30.06
30.08
30.10
30.18
30.14
30.
TIME

2

JPL WT 20-499

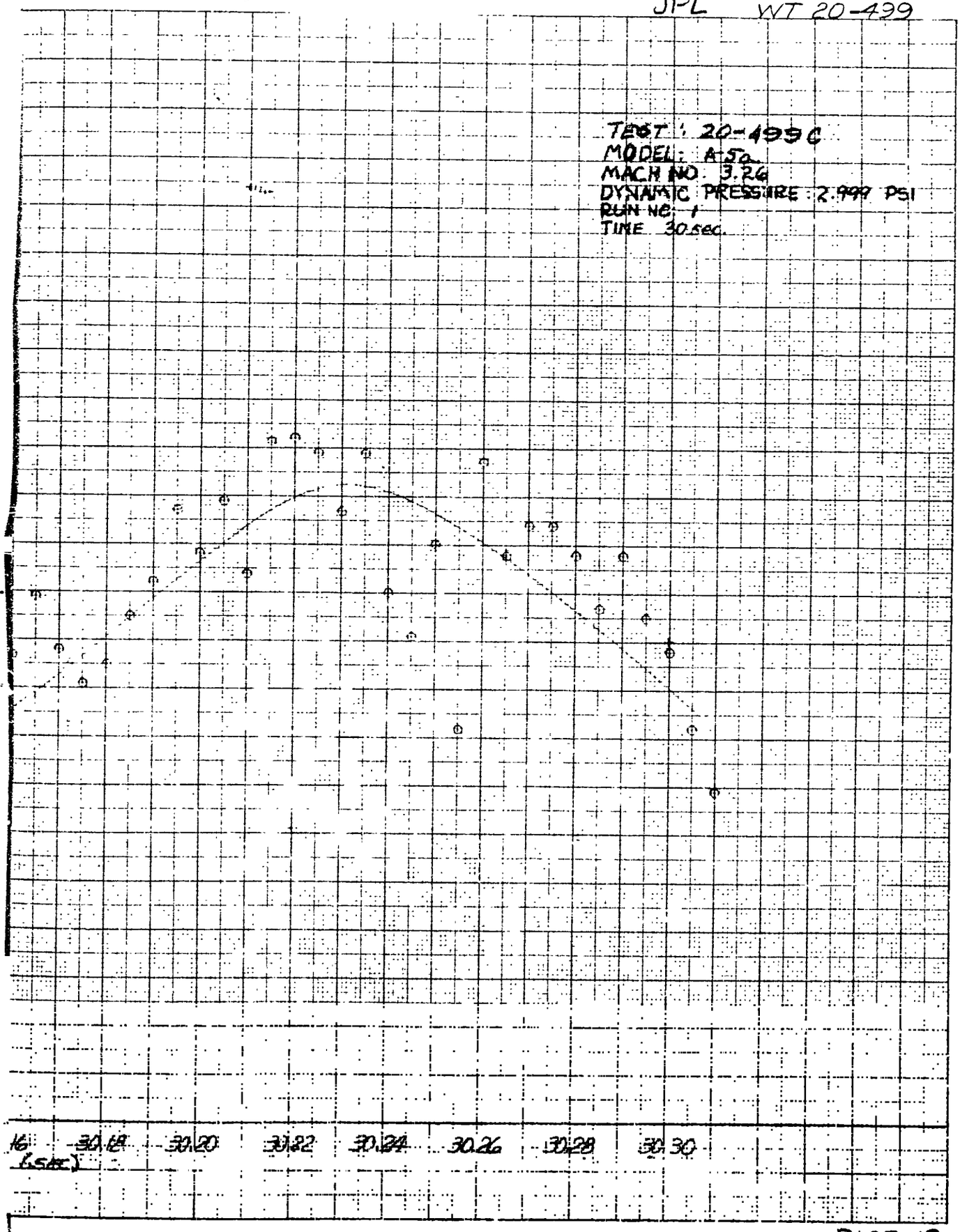

PLOT 18

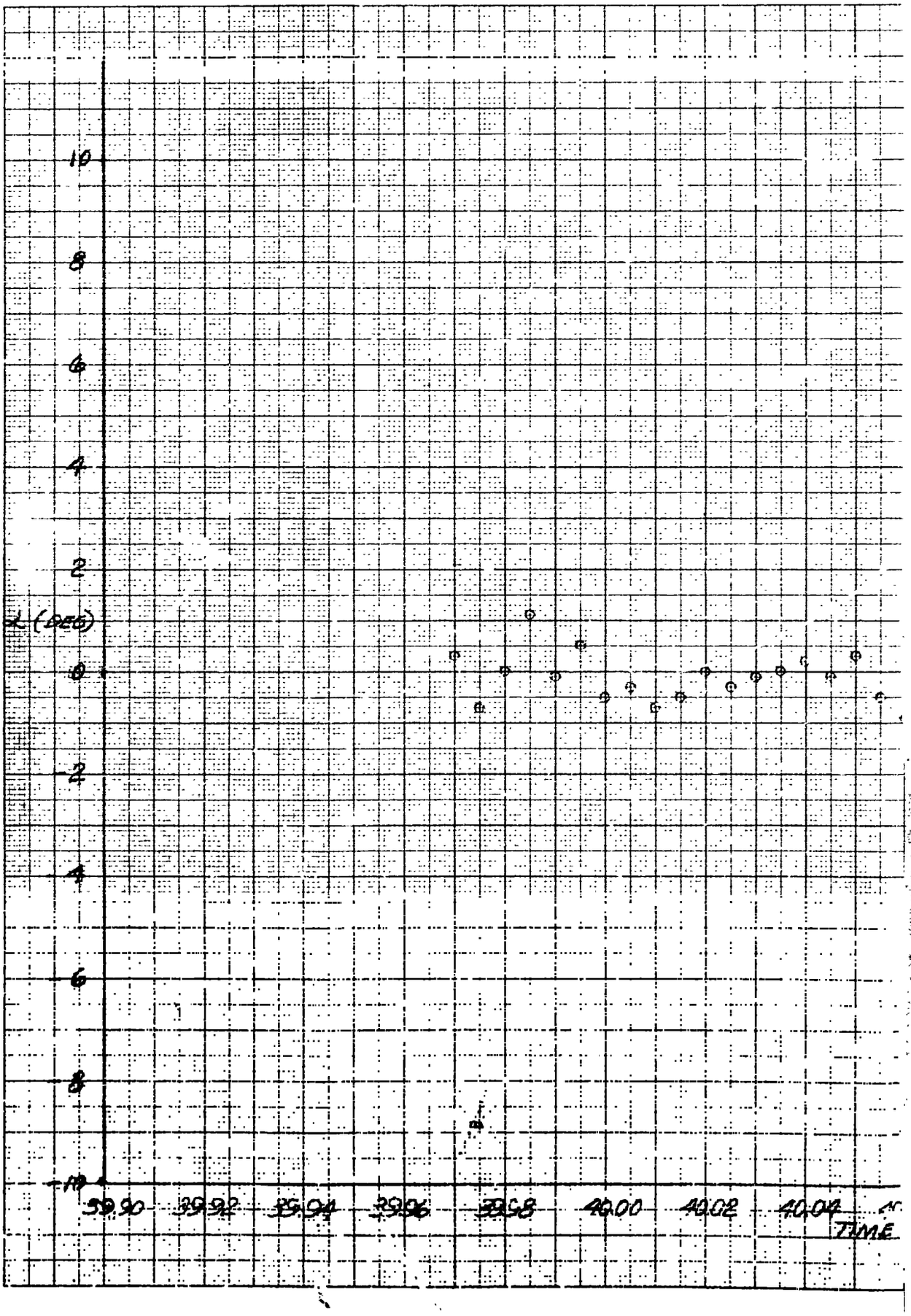
10
8
6
4
2
0
-2
-4
-6
-8
-10
39.90
39.92
39.94
39.96
39.98
40.00
40.02
40.04
TIME

7

JPL WT 20-499

TEST: 20-499C
MODEL: A-5a
MACH NO: 3.26
DYNAMIC PRESSURE: 2.999 PSI
RUN NO: 1
TIME: 40 SEC

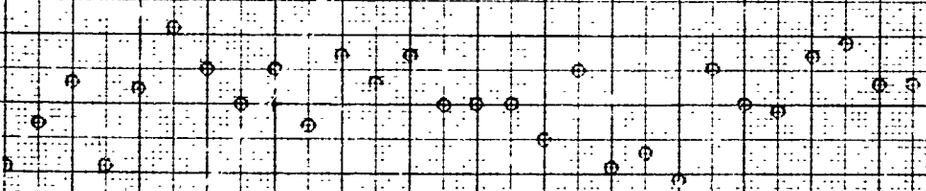

40.06 40.08 40.10 40.12 40.14 40.16 40.18 40.20
(SEC)

PLOT 19

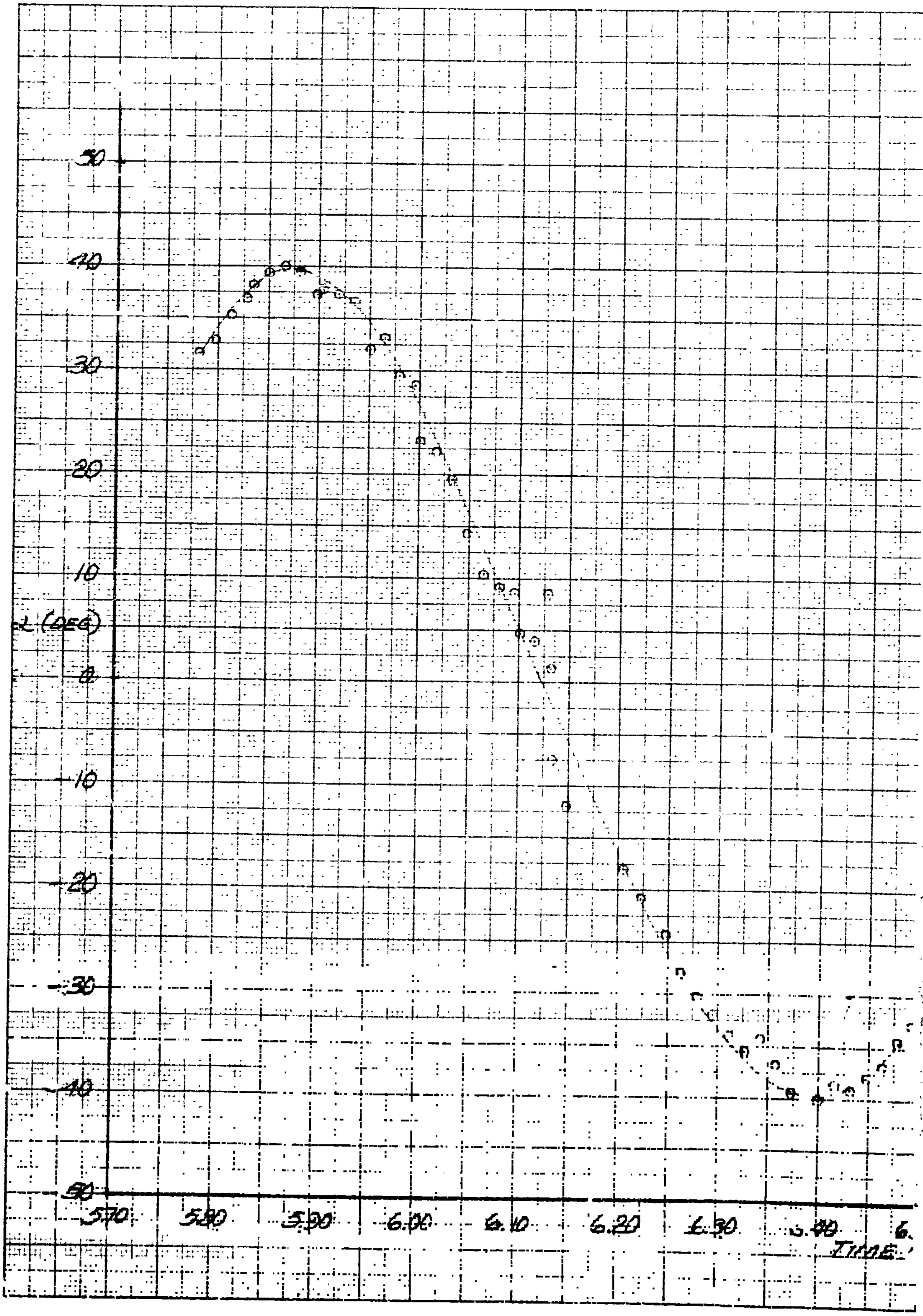

2

JPL WT 20-499

TEST: 20-516
MODEL: C.S.
MACH NO: 3.26
DYNAMIC PRESSURE: 3.158 PSI
RUN NO: 33
TIME: 6 sec.

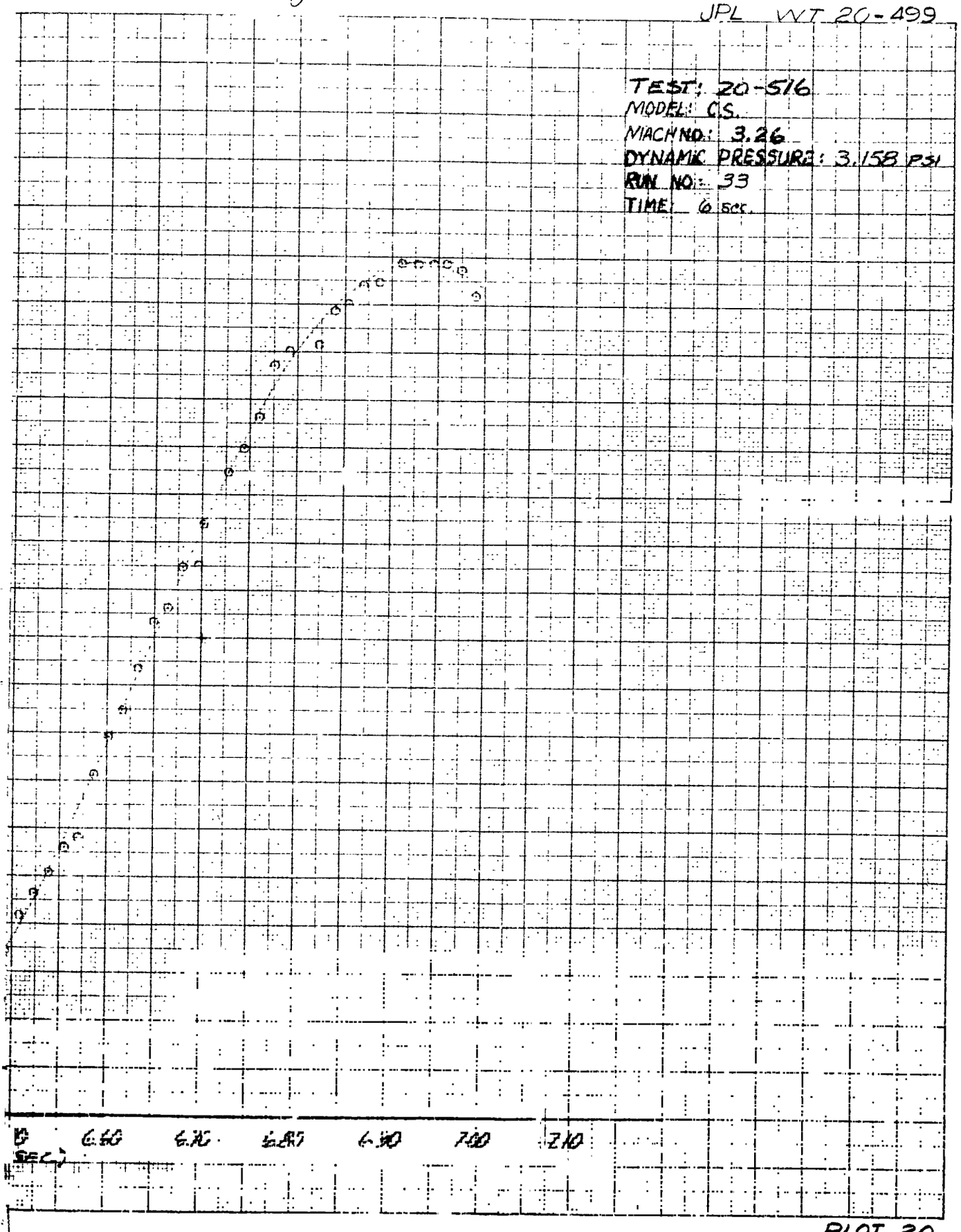

PLOT 20

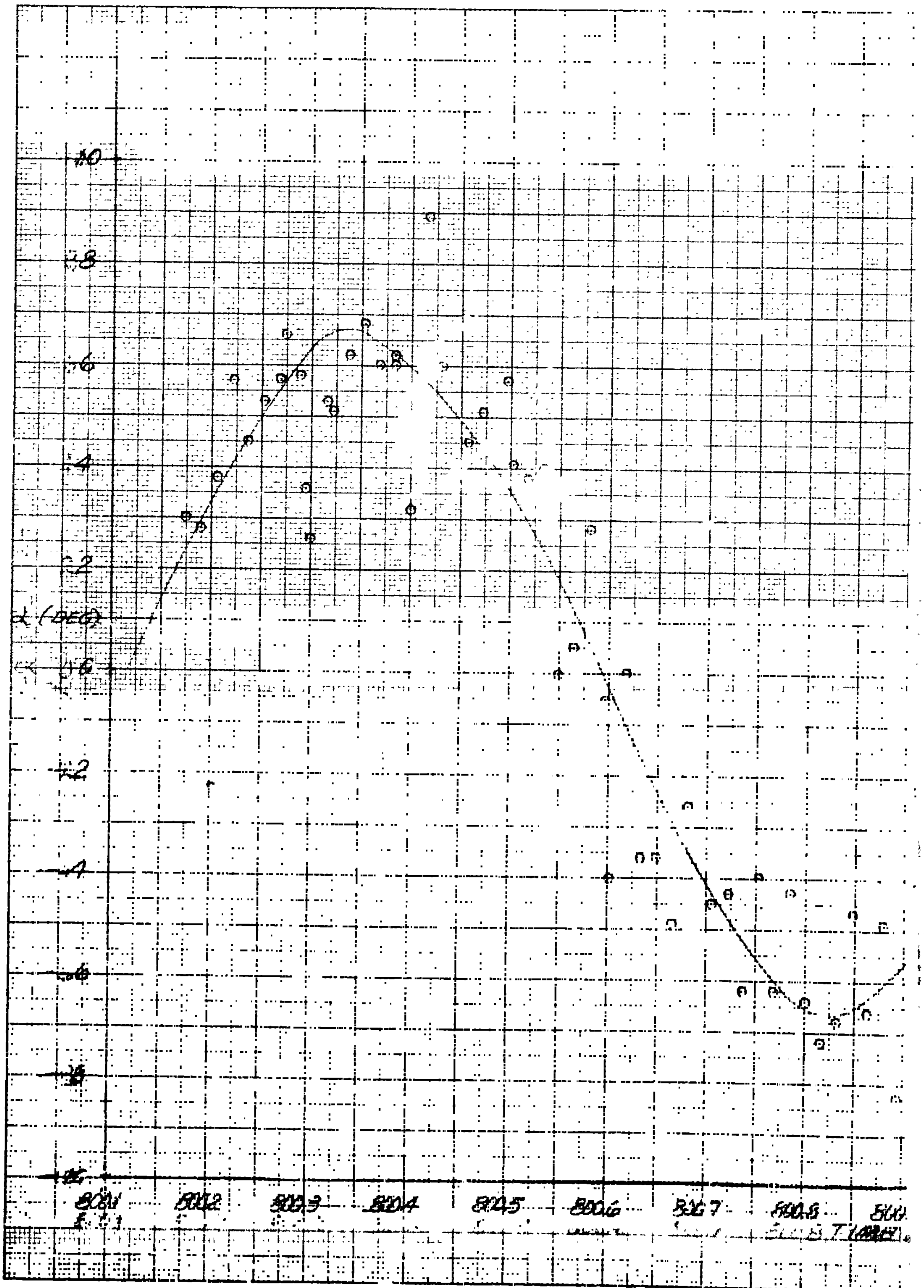

2

JPL WT 20-499

TEST: 20-516
MODEL: C.S.
MACH NO: 3.46
DYNAMIC PRESSURE: 3.158 PSI
RUN NO: 33
TIME 800 SEC

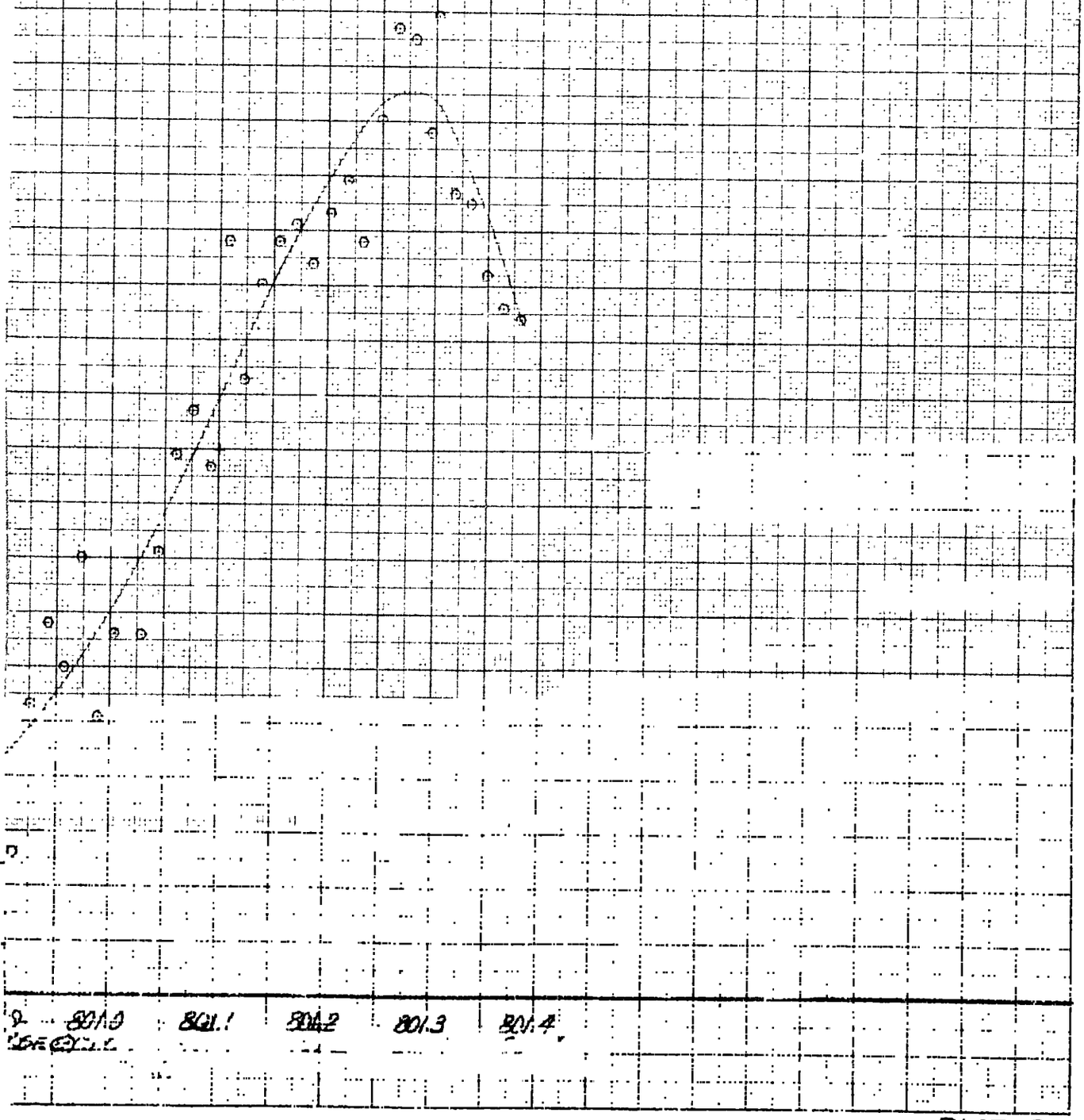

801.0 801.1 801.2 801.3 801.4

PLOT 21

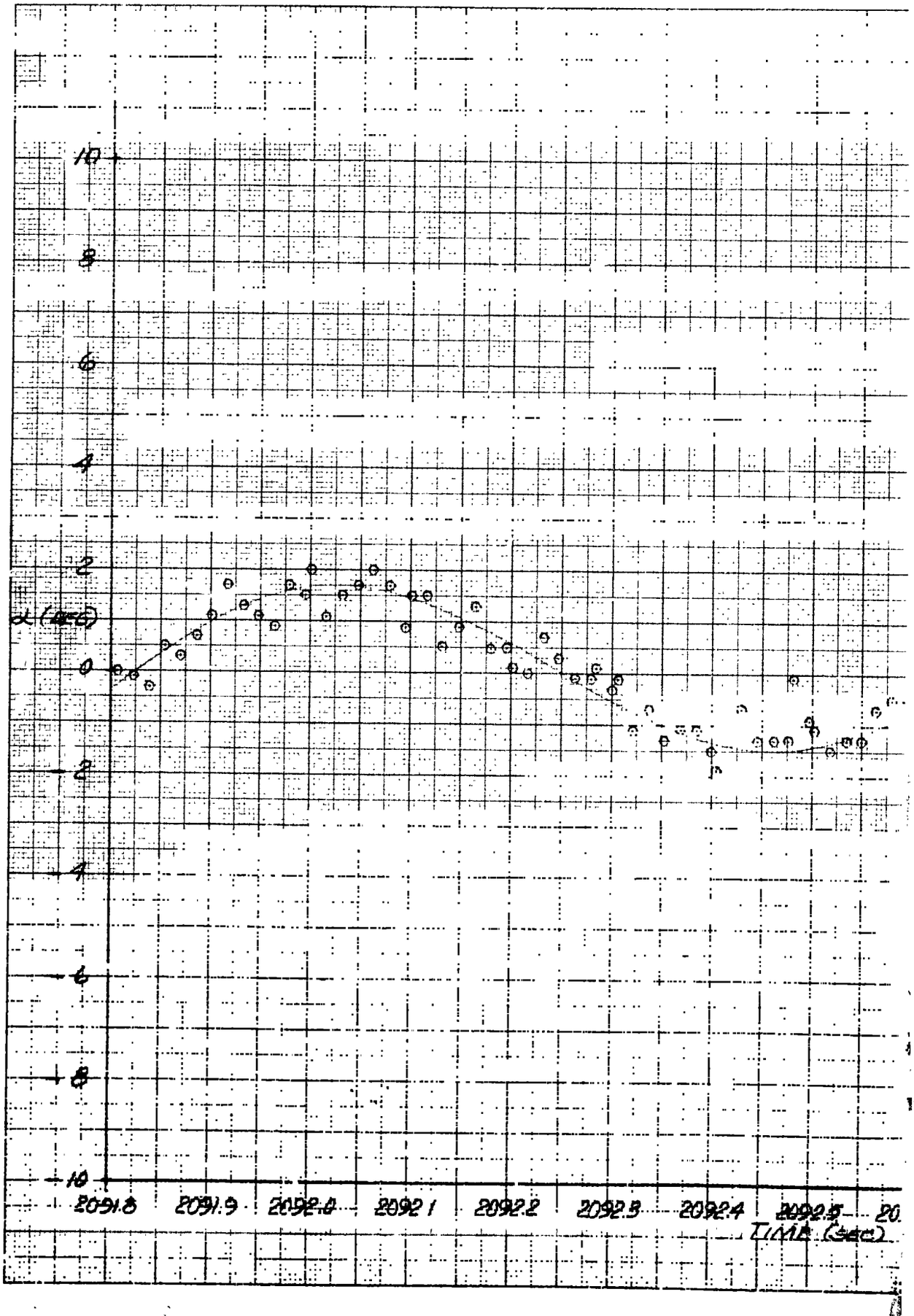
10
8
6
4
2
0
−2
−4
−6
−8
−10
2091.8
2091.9
2092.0
2092.1
2092.2
2092.3
2092.4
2092.5
TIME (Sec)

2

JPL WT 20-499

TEST:	20-516
MODEL:	C.S.
MACH NO.	3.26
DYNAMIC PRESSURE	3.108 PSI
RUN NO.	33
TIME:	2092 sec.

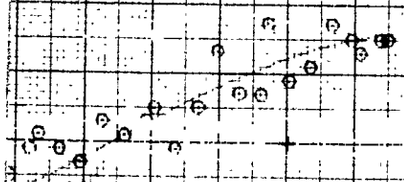

20926 20927 20928 20929 20930

PLOT 22

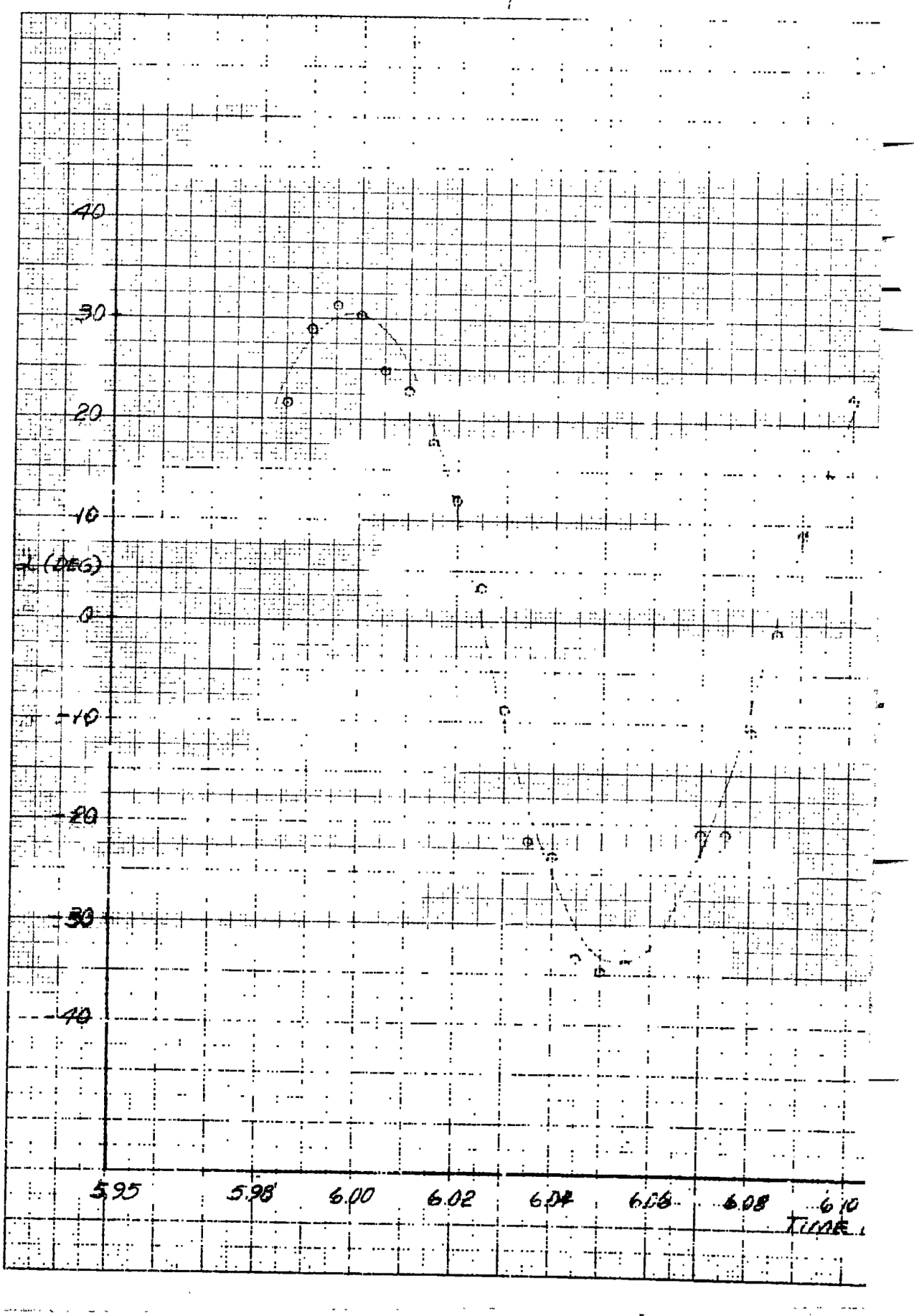
40
30
20
10
0
-10
-20
-30
-40
γ (DEG)
5.95
5.98
6.00
6.02
6.04
6.06
6.08
6.10
TIME

2

JPL WT 20-499

TEST: 20-499C
MODEL: A-5a
MACH NO: 1.81
DYNAMIC PRESSURE: 3.028 Psi
RUN NO: 5
TIME 6 sec.

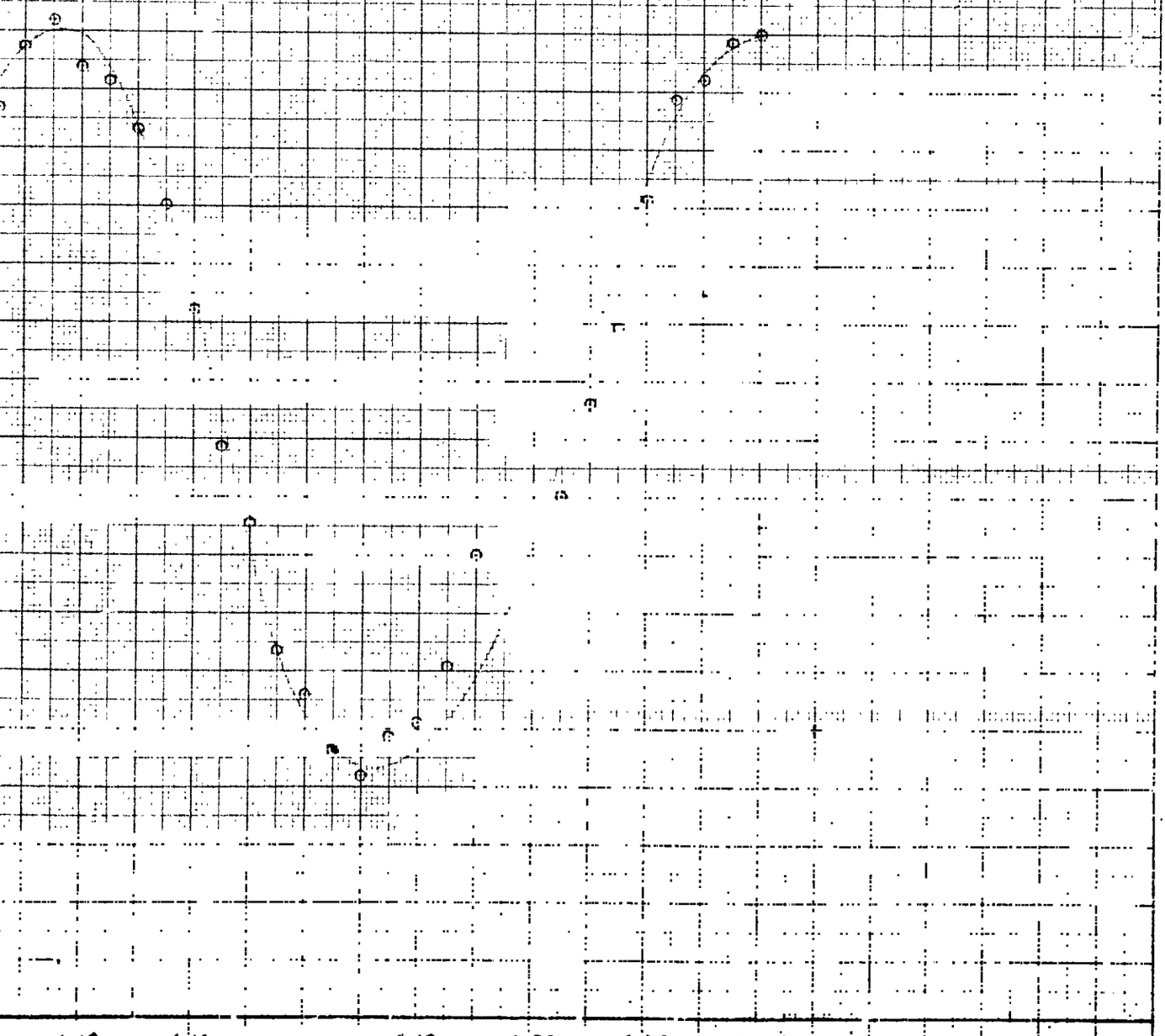

PLOT 23

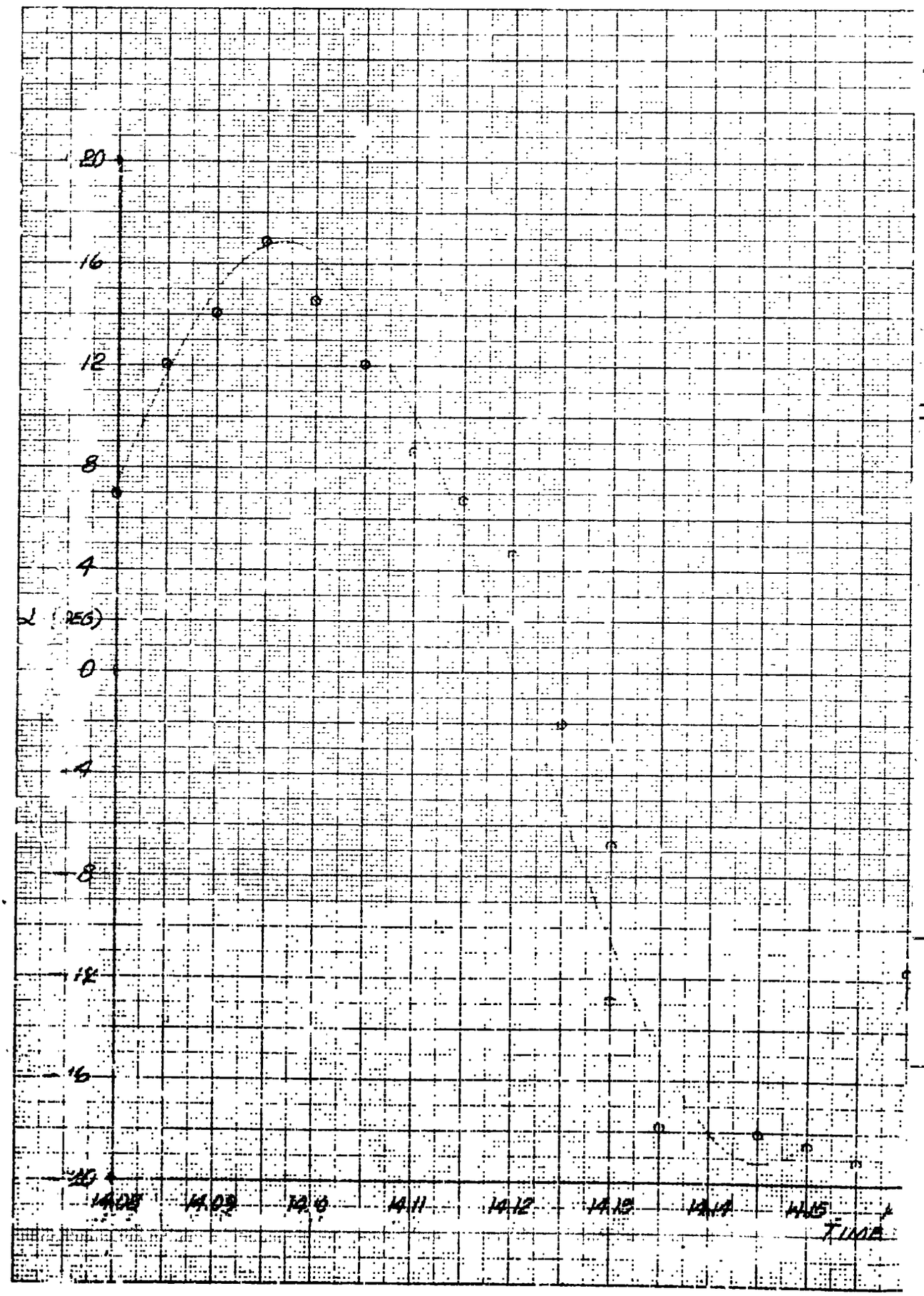
20
16
12
8
4
L (DEG)
0
-4
-8
-12
-16
-20
14:08
14:09
14:10
14:11
14:12
14:13
14:14
14:15
TIME

2

JPL WT 20-499

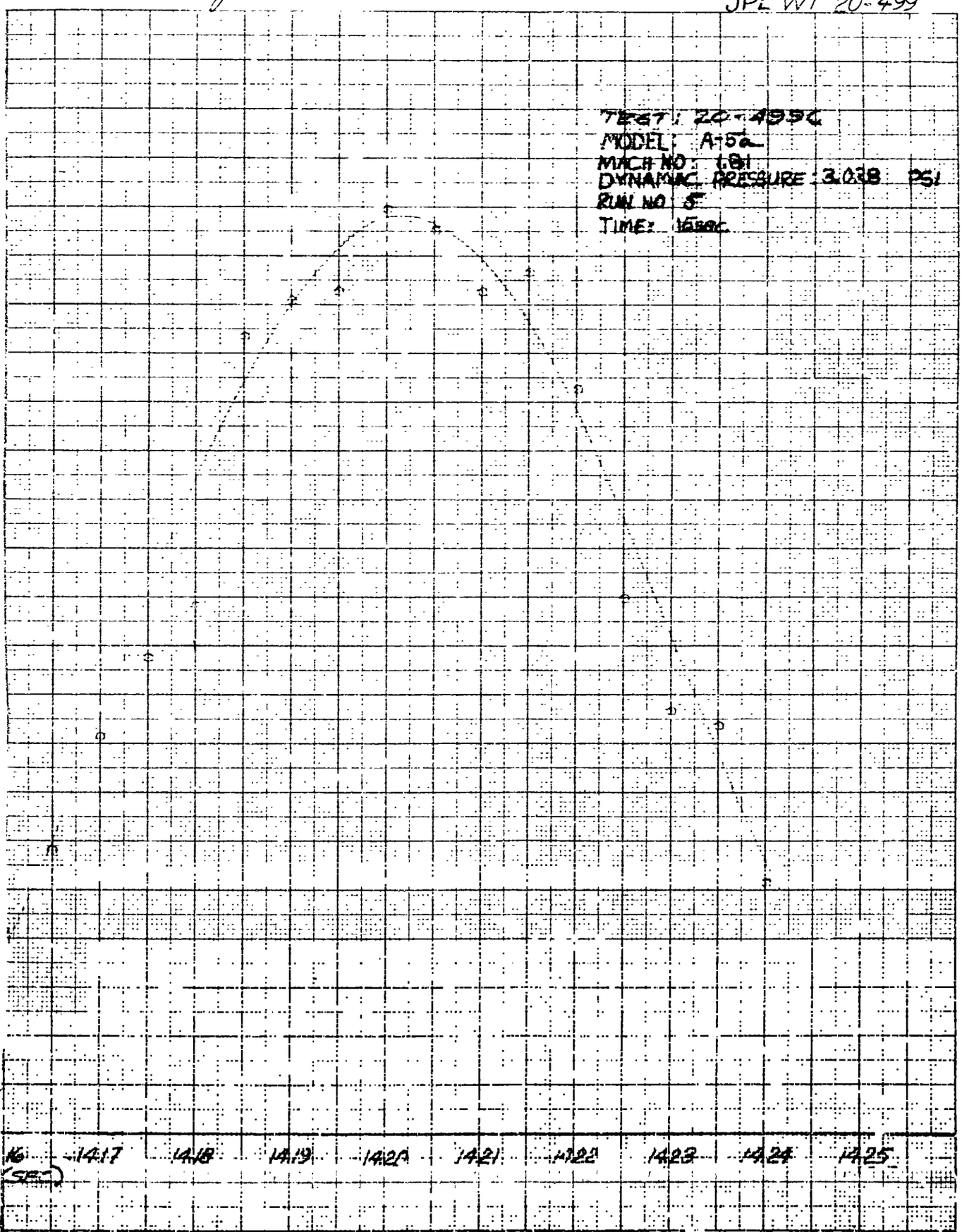

PLOT 24

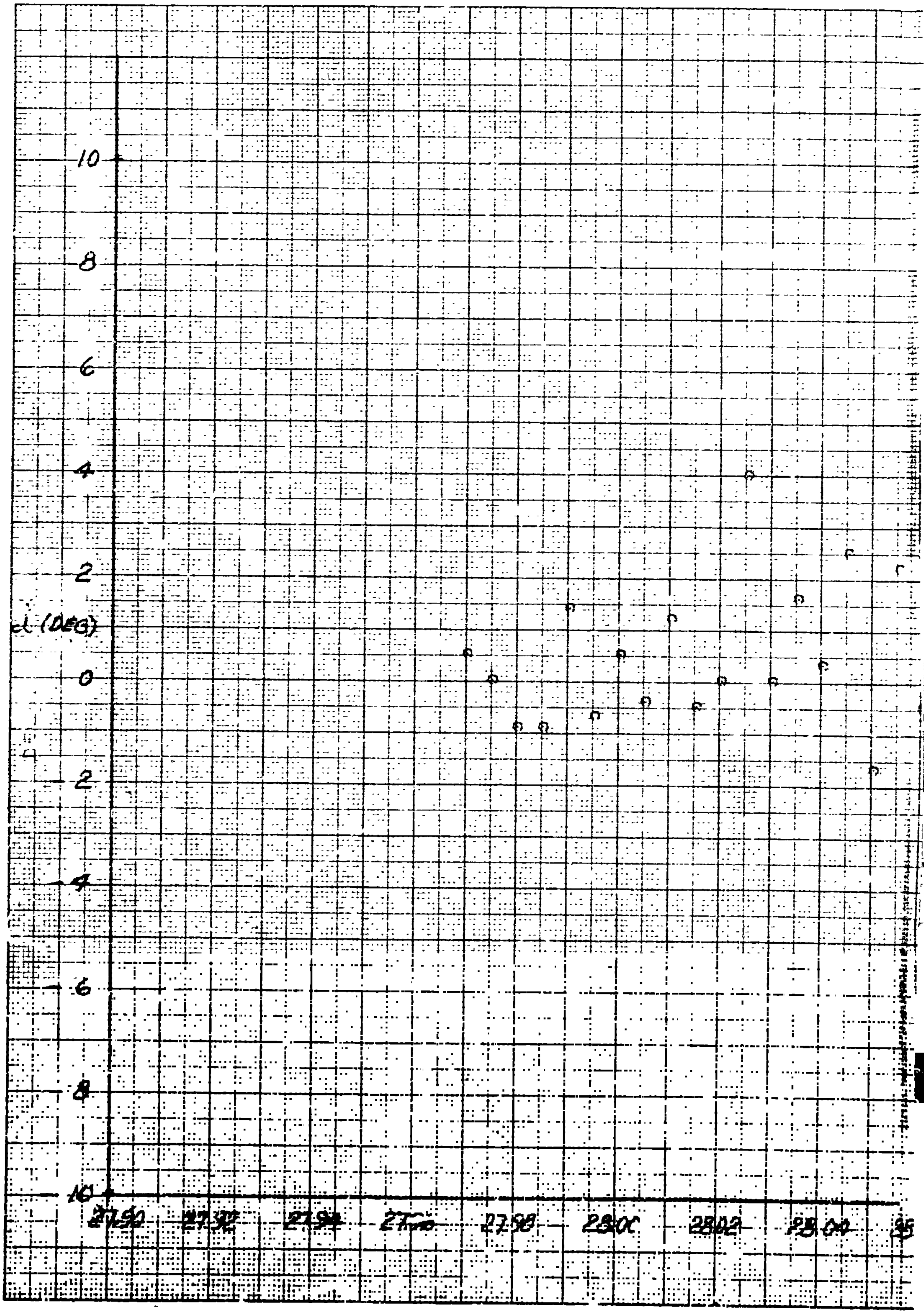

1

JPL WT 20-499

TEST:	20-499C
MODEL:	A-5a
MACH NO:	1.81
DYNAMIC PRESSURE:	3.028
RUN NO.	5
TIME:	28 SEC

28.06 28.08 28.10 28.12 28.14 28.16 28.18 28.20 28.22

TIME (SEC)

PLOT 25

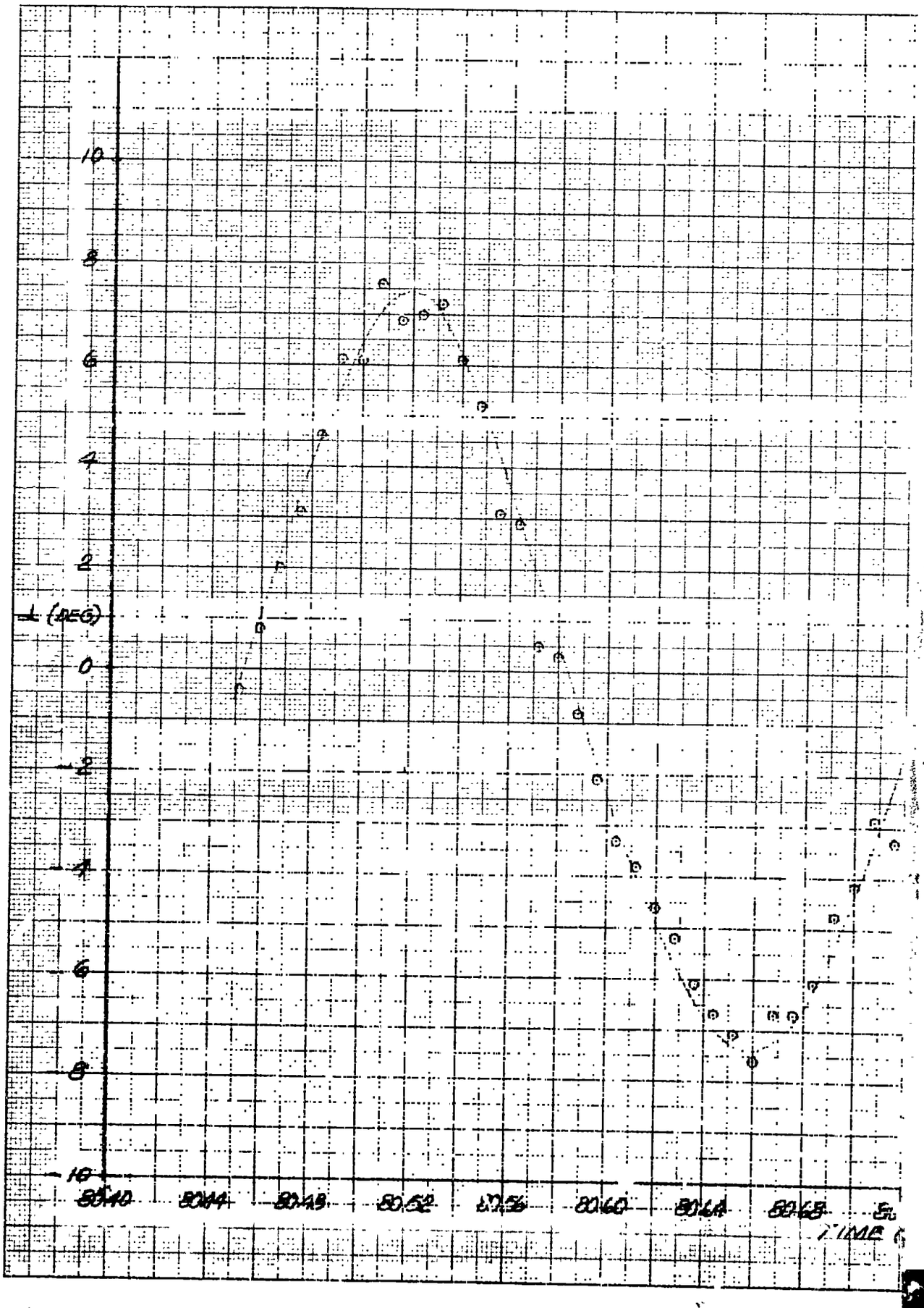
10
8
6
4
2
0
-2
-4
-6
-8
-10
TIME

2

JPL WT 20-499

TEST:	21-106A
MODEL:	A-5a
MACH NO.	5.95
DYNAMIC PRESSURE	1.686 PSI
RUN NO.	3
TIME:	1805~~04~~

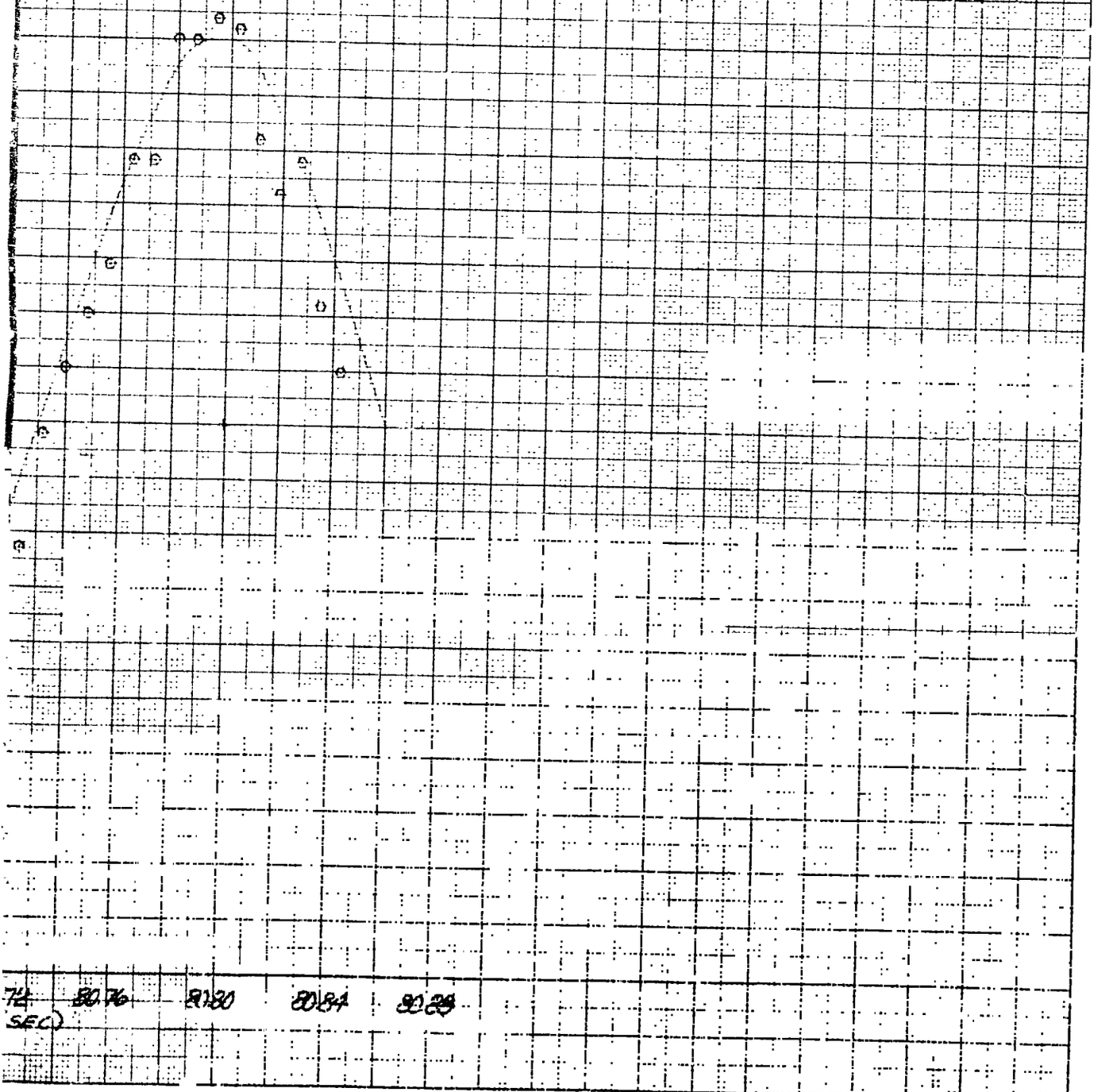

74 80 76 80 80 80 84 80 88
SEC)

PLOT 21

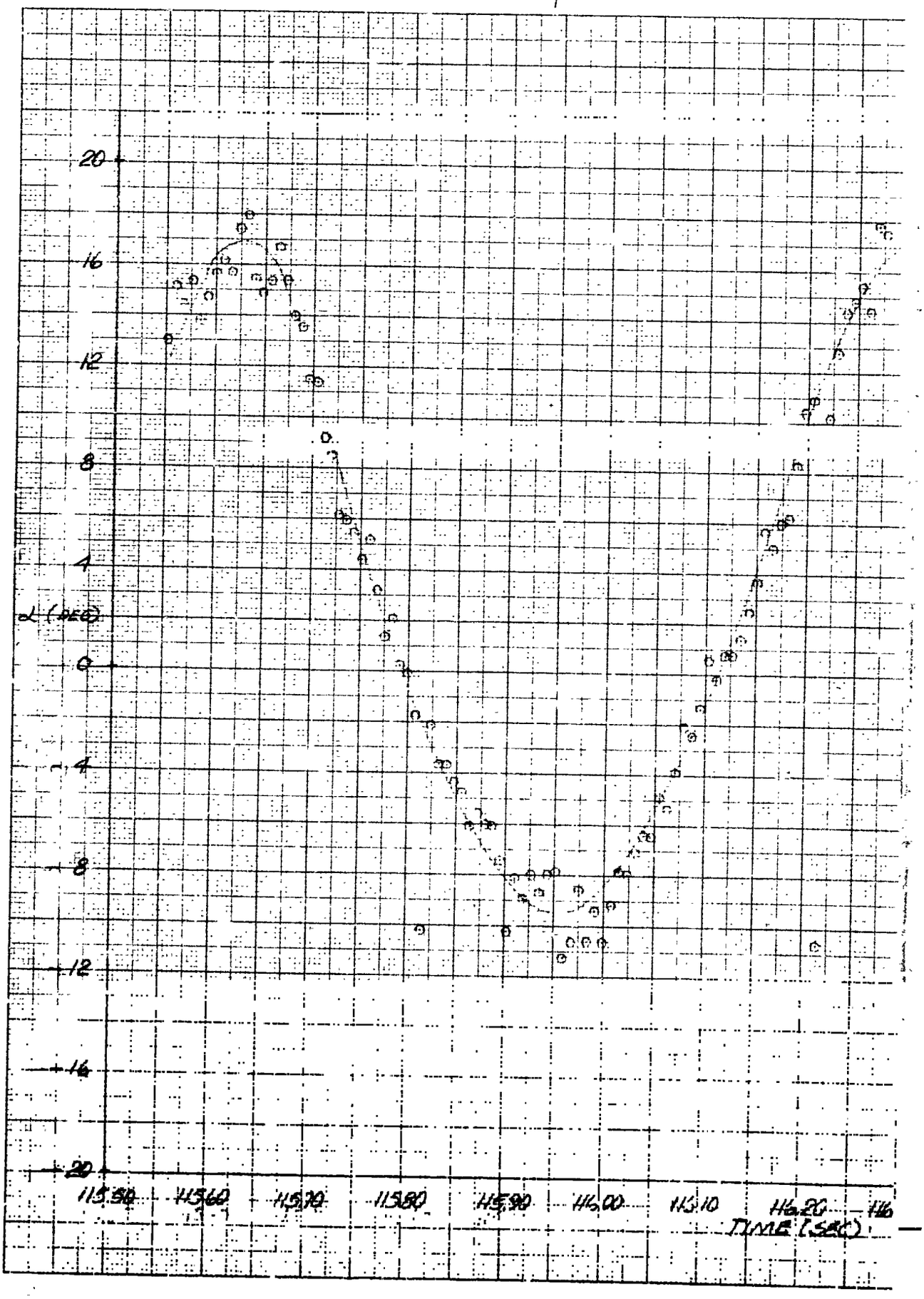
20
16
12
8
4
0
4
8
12
16
20
α (DEG)
115.50
115.60
115.70
115.80
115.90
116.00
116.10
116.20
116
TIME (SEC)

2

JPL. WT 20-499

TEST: 21-106A
MODEL: A-5a
MACH NO: 5.95
DYNAMIC PRESSURE: 1.686 PSI
RUN NO: 3
TIME: 116 sec.

30 | 116.40 | 116.50 | 116.60 | 116.70

PLOT 27

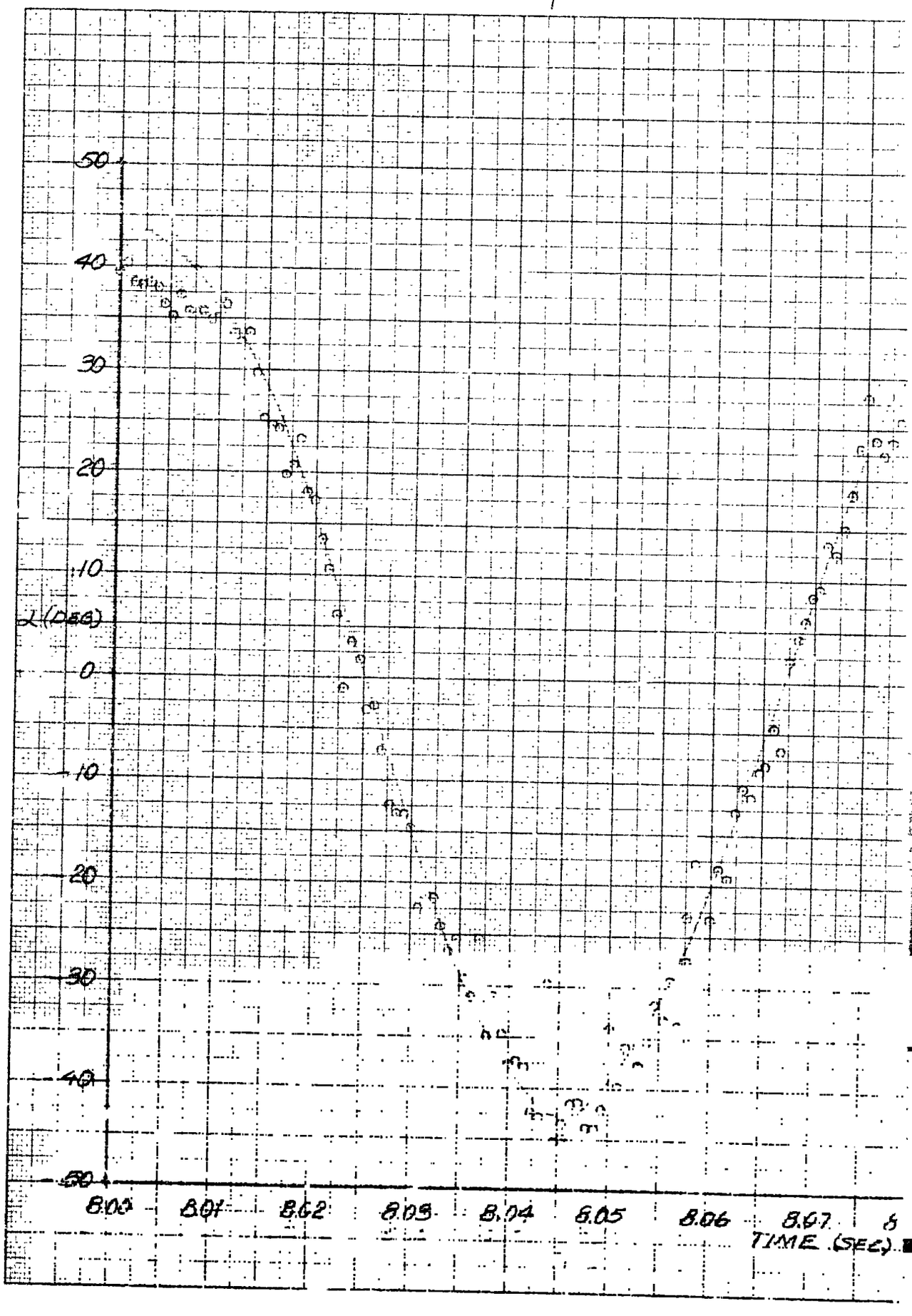
50
40
30
20
10
L (DEG)
0
10
20
30
40
50
8.00
8.01
8.02
8.03
8.04
8.05
8.06
8.07
TIME (SEC)

2

JPL WT 20-499

TEST : 21-106B
MODEL : CS.
MACH NO : 6.07
DYNAMIC PRESSURE : 2.870 PSI
RUN NO : 6
TIME : 8 sec.

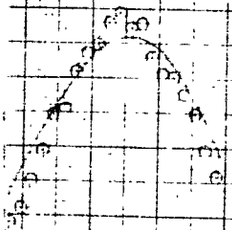

8.08 8.09 8.10 8.11 8.12

PLOT 28

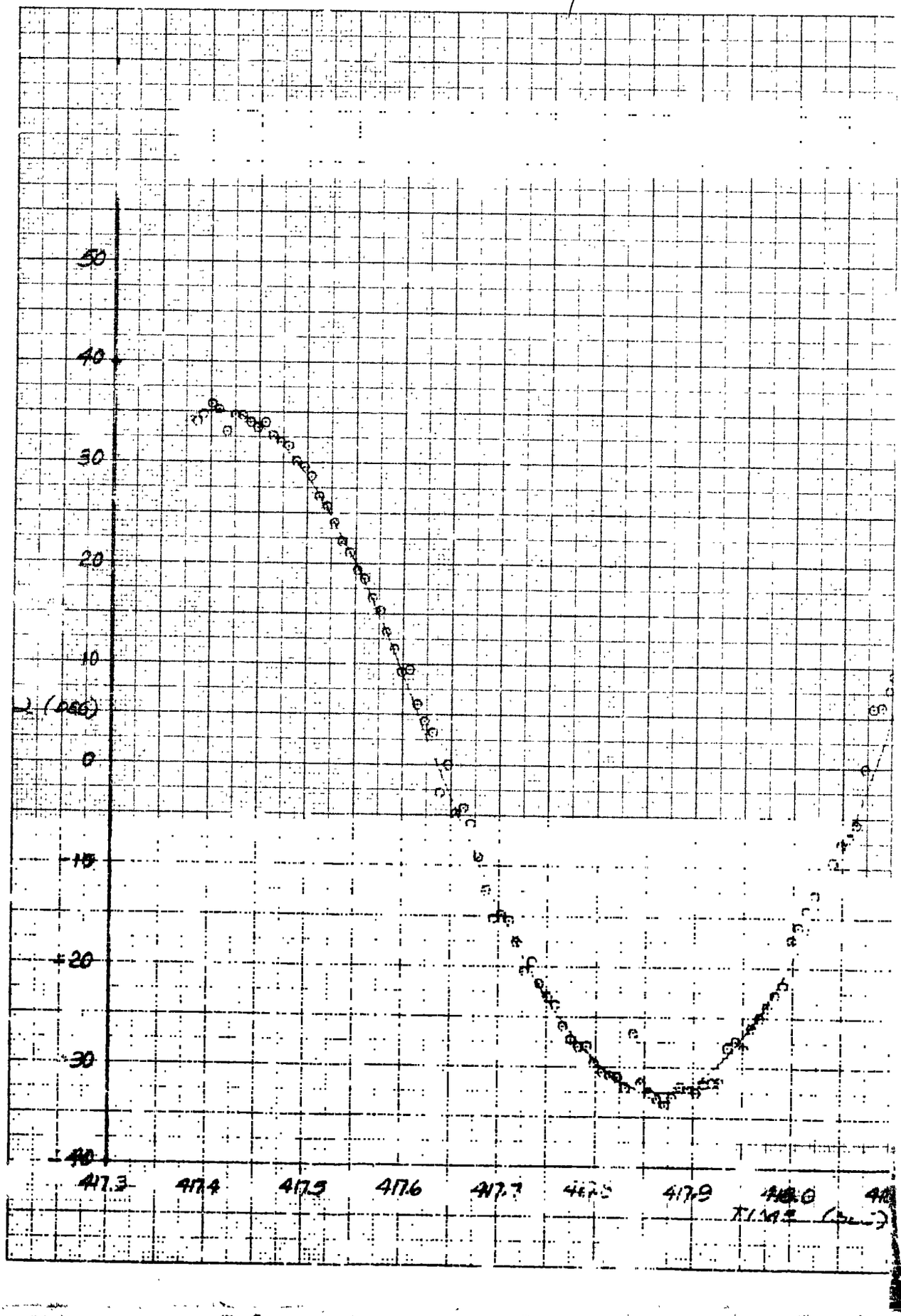
50
40
30
20
10
0
10
20
30
40
417.3
417.4
417.5
417.6
417.7
417.9

2

JPL WT 20-499

TEST: 21-106B
MODEL: C.5.
MACH NO. 6.07
DYNAMIC PRESSURE: 2.870 psi
RUN NO: 6
TIME: 417 SEC

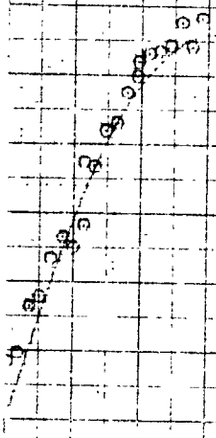

Bit 418.2 418.3 418.4

PLOT 29

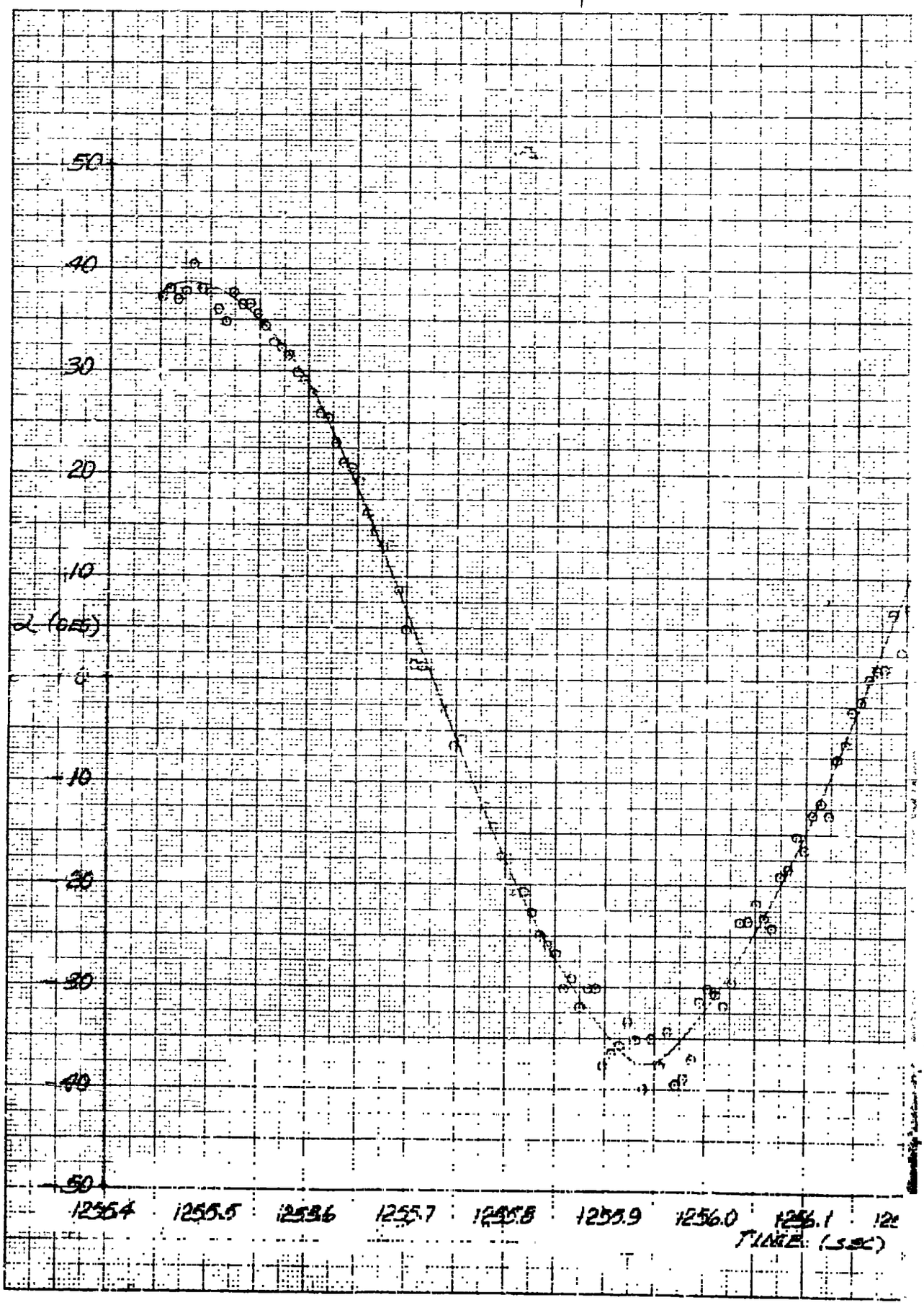
50
40
30
20
10
0
-10
-20
-30
-40
-50
L (DEG)
12554
1255.5
1255.6
1255.7
1255.8
1255.9
1256.0
1256.1
TIME (SEC)

2

JPL WT 20-499

TEST: 21-1063
MODEL: C-5,
MACH NO.: 6.07
DYNAMIC PRESSURE: 2.870 psi
RUN NO: 6
TIME: 1255 sec

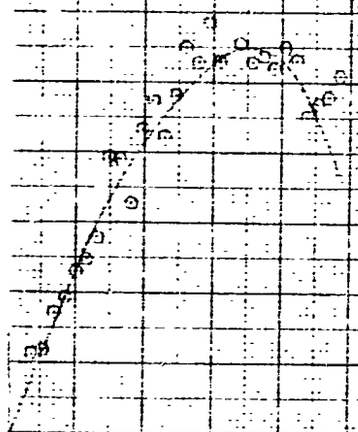

Vac 1256.3 1256.4 1256.5

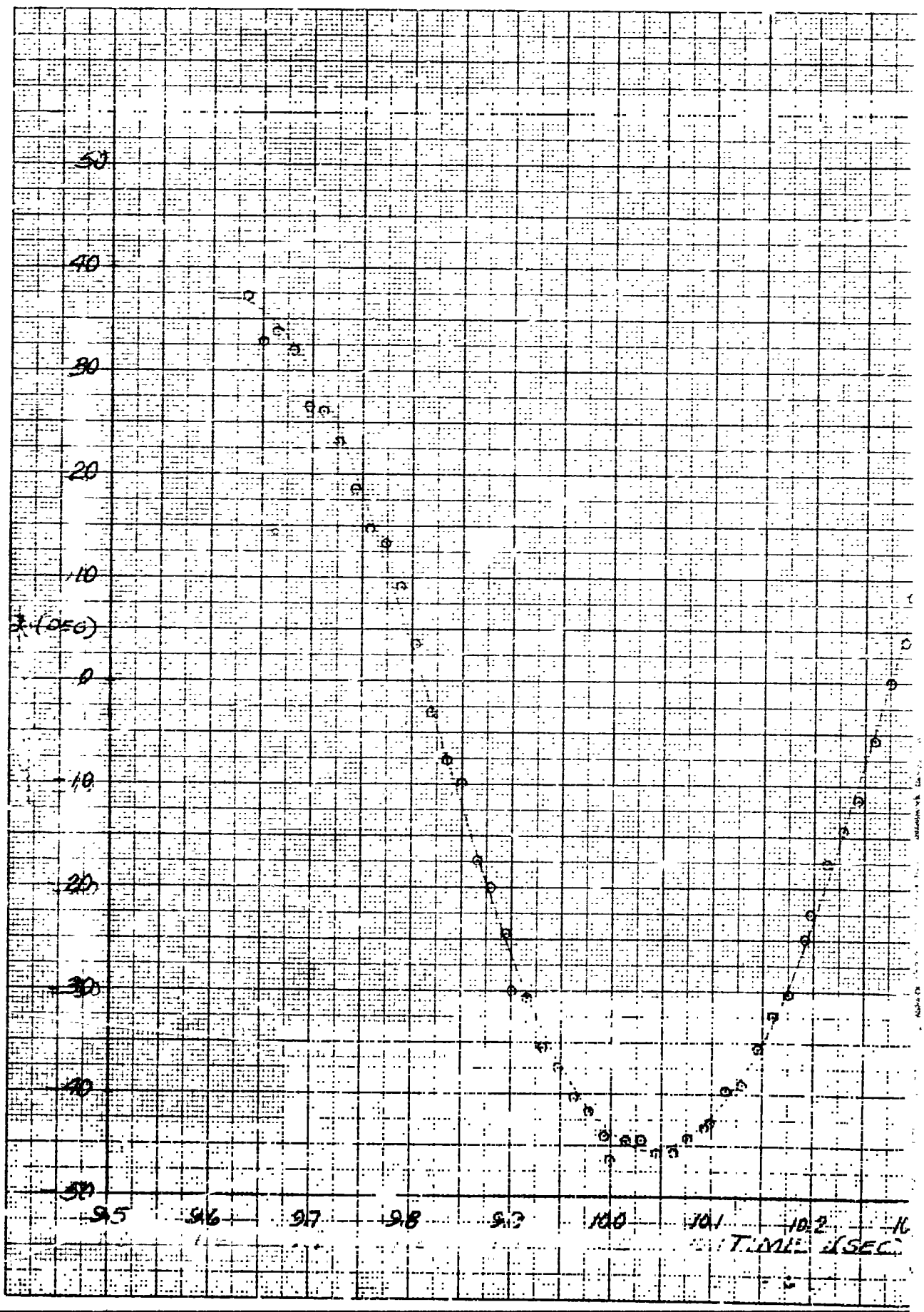
50
40
30
20
10
0
10
20
30
40
50
95
96
97
98
99
100
101
102
TIME (SEC)

2

JPL WT 20-499

TEST: 21-13
MODEL: C.5
MACH NO: 6.12
DYNAMIC PRESSURE: 2.554 PSI
RUN NO: 16
TIME 10sec.

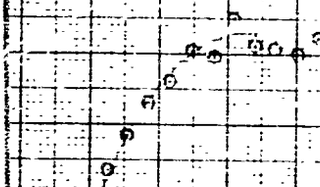

3 144 145 146

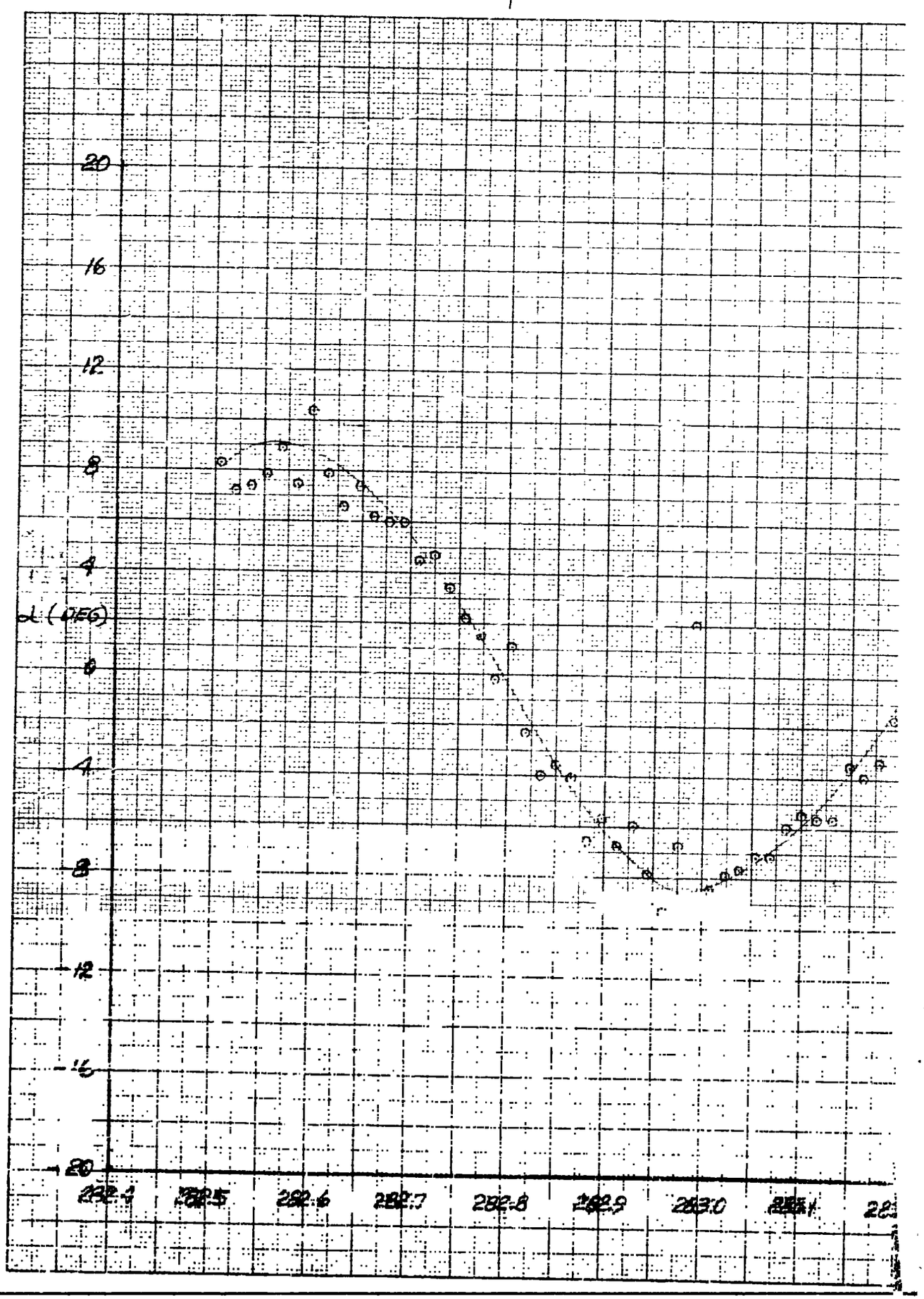
20
16
12
8
4
α (DEG)
0
4
8
12
16
20
282.4
282.5
282.6
282.7
282.8
282.9
283.0

9

JPL WT 20-499

TEST : 21-113
MODEL : C-5
MACH NO : 6.12
DYNAMIC PRESSURE : 2.537 psi
RUN NO : 16
TIME : 282 SEC

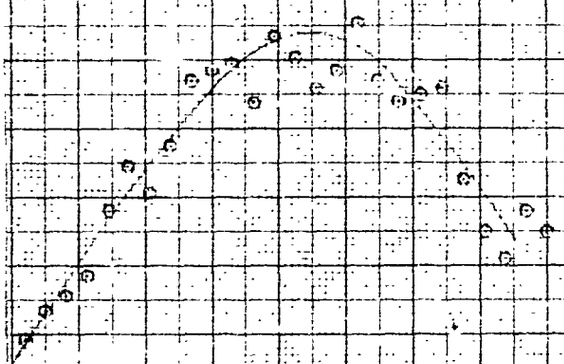

.2 283.3 283.4 283.5 283.6 283.7 283.8
TIME (SEC)

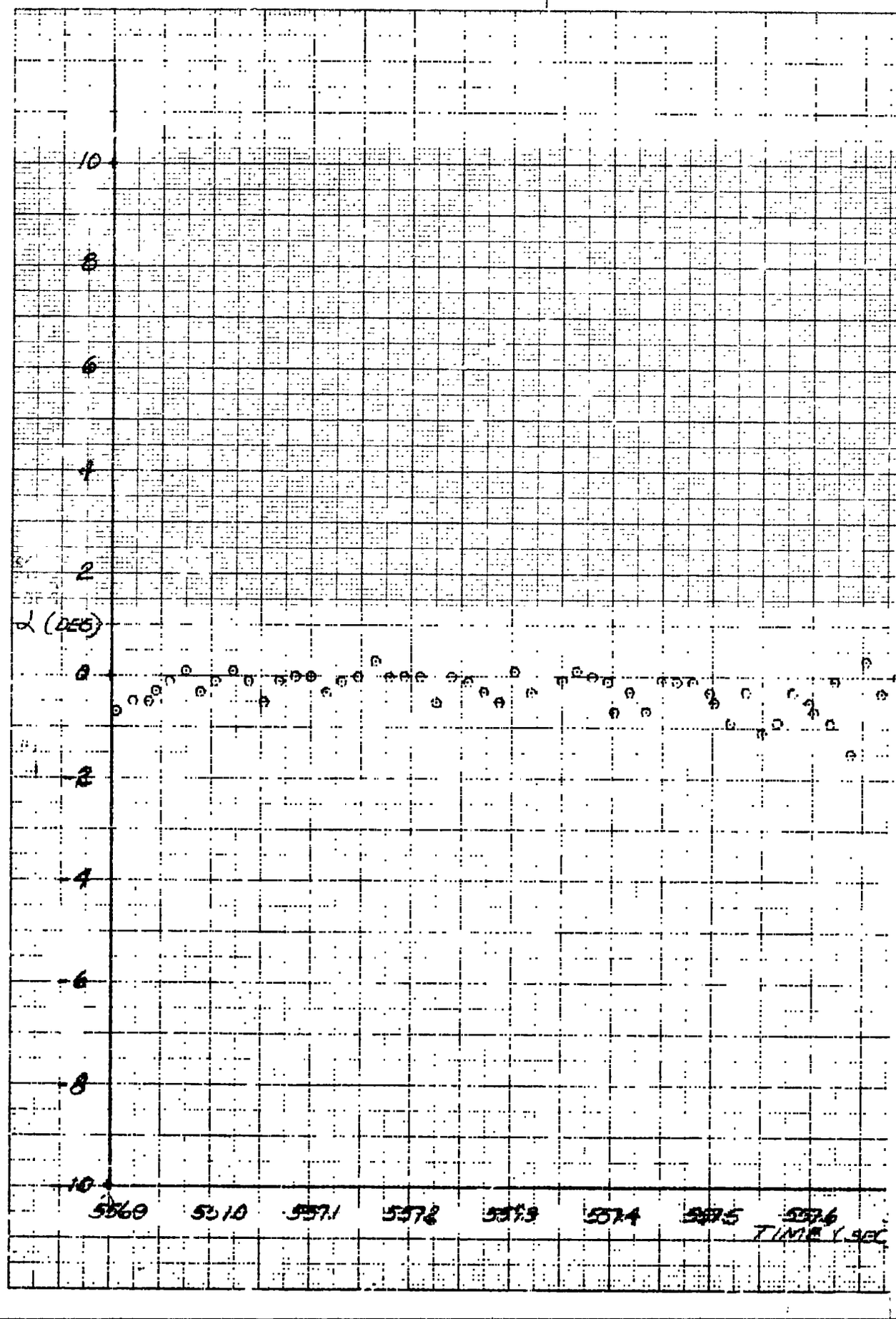
10
8
6
4
2
0
-2
-4
-6
-8
-10
5560
5570
5571
5572
5573
5574
5575
5576
TIME (SEC)

2

JPL WT 20-499

TEST: 27-W3
MODEL: C.5.
MACH NO: 6.12
DYNAMIC PRESSURE: 2.654 PSI
RUN NO. 16
TIME: 557 SEC

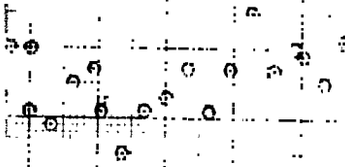

527 538 537.9 539.0

JPL WT 20-499

TEST	RUN	MACH	MODEL	q (PSIA)	MOMENT OF INERTIA (IN-LB-SEC²)
20-465	○ 7.8	2.01	A-2	2.605	0.0156
20-465	□ 8.2	3.01	A-2	2.654	0.0156

△ ESTIMATED BALL BEARING DAMPING AT M = 3.0

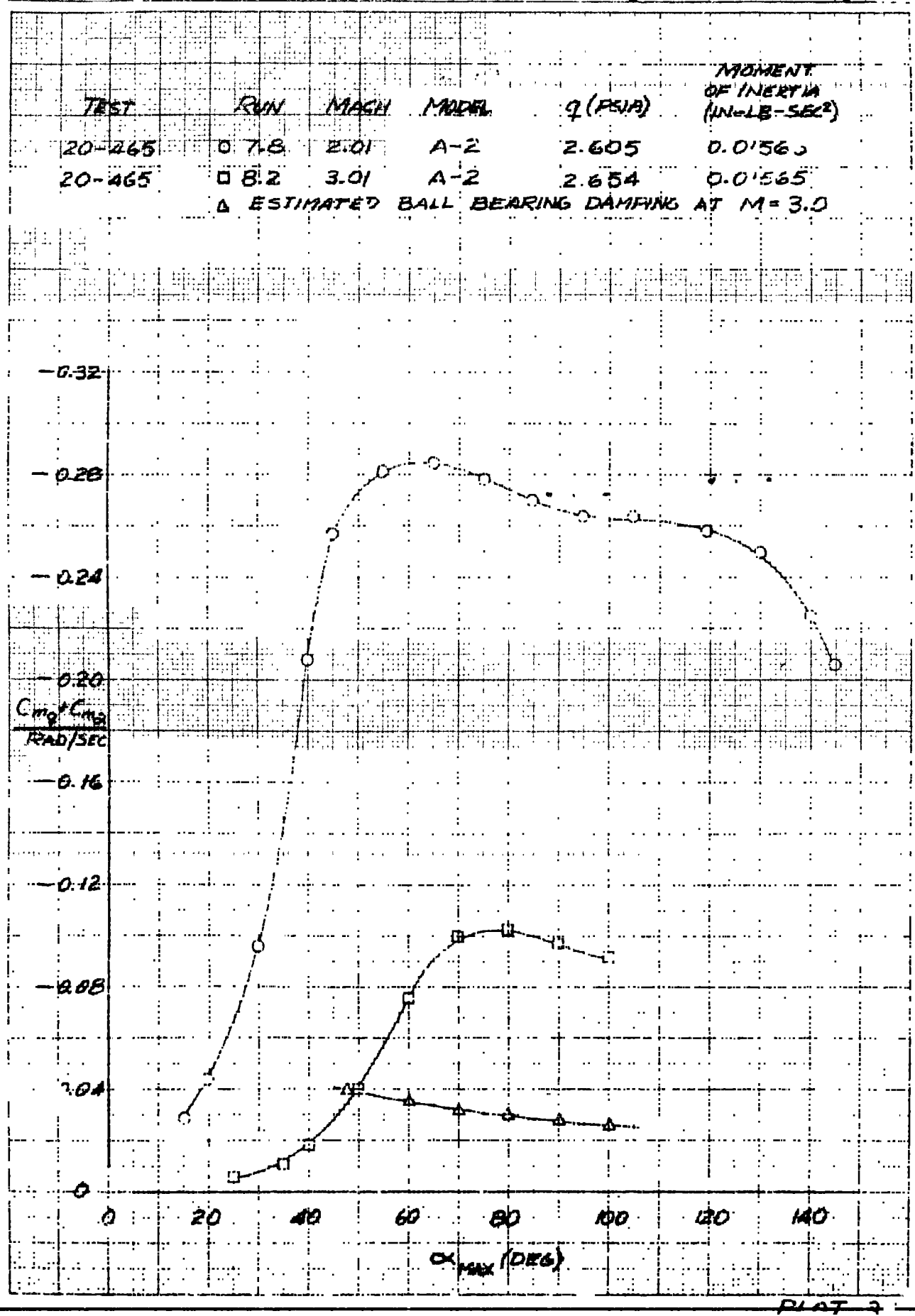

PLOT 2